



Atmosphere and Ocean Origins of North American Droughts*

RICHARD SEAGER

Lamont-Doherty Earth Observatory, Columbia University, Palisades, New York

MARTIN HOERLING

NOAA/Earth System Research Laboratory, Boulder, Colorado

(Manuscript received 6 June 2013, in final form 3 March 2014)

ABSTRACT

The atmospheric and oceanic causes of North American droughts are examined using observations and ensemble climate simulations. The models indicate that oceanic forcing of annual mean precipitation variability accounts for up to 40% of total variance in northeastern Mexico, the southern Great Plains, and the Gulf Coast states but less than 10% in central and eastern Canada. Observations and models indicate robust tropical Pacific and tropical North Atlantic forcing of annual mean precipitation and soil moisture with the most heavily influenced areas being in southwestern North America and the southern Great Plains. In these regions, individual wet and dry years, droughts, and decadal variations are well reproduced in atmosphere models forced by observed SSTs. Oceanic forcing was important in causing multiyear droughts in the 1950s and at the turn of the twenty-first century, although a similar ocean configuration in the 1970s was not associated with drought owing to an overwhelming influence of internal atmospheric variability. Up to half of the soil moisture deficits during severe droughts in the southeast United States in 2000, Texas in 2011, and the central Great Plains in 2012 were related to SST forcing, although SST forcing was an insignificant factor for northern Great Plains drought in 1988. During the early twenty-first century, natural decadal swings in tropical Pacific and North Atlantic SSTs have contributed to a dry regime for the United States. Long-term changes caused by increasing trace gas concentrations are now contributing to a modest signal of soil moisture depletion, mainly over the U.S. Southwest, thereby prolonging the duration and severity of naturally occurring droughts.

1. Introduction

In a nation that has been reeling from one weather or climate disaster to another, with record tornado outbreaks, landfalling tropical storms and superstorms, record winter snowfalls, and severe floods, persistent droughts appear almost prosaic. Droughts do not cause the mass loss of life and property destruction by floods and storms. They are instead slow-motion disasters whose beginnings and ends are even often hard to

identify. However, while the social and financial costs of hurricane, tornado, and flood disasters are, of course, tremendous, droughts are one of the costliest of natural disasters in the United States. Much of that cost is related to crop failure but droughts can also lead to spectacular events in the form of wildfires and the costs of fighting these are immense. Further, crop failures easily translate into spikes in food prices, given the global food market across the world. In one truly exceptional case—the 1930s Dust Bowl—drought led to millions in the Great Plains leaving their homes, hundreds of thousands migrating from the region, an unknown number of deaths from dust pneumonia, and a permanent transformation in the agriculture, economy, and society of the region and the wider nation (Worster 1979). U.S. droughts more often than not appear as components of droughts that also impact Mexico and/or Canada. For example, the 1950s U.S. Southwest

*Lamont-Doherty Earth Observatory Contribution Number 7786.

Corresponding author address: Richard Seager, Lamont-Doherty Earth Observatory, Columbia University, 61 Route 9W, Palisades, NY 10964.
E-mail: seager@ldeo.columbia.edu

drought was also one of the worst that Mexico has experienced, and Mexico has been struggling with ongoing drought since the mid-1990s (Seager et al. 2009b; Stahle et al. 2009). Further, the 1998 to 2004 drought in the United States—which, for example, dropped Colorado River storage to record lows—also severely impacted much of Canada (Stewart and Lawford 2011; Bonsal et al. 2011). Given these transcontinental and multinational consequences of drought, considerable effort has been expended in an attempt to understand why they occur and whether they can be predicted in advance. In recent years an increasing amount of this research effort has focused on whether, where, and when droughts in the United States will become more common or severe due to climate change caused by rising greenhouse gases.

Despite years of study, progress in understanding the causes of North American droughts only made serious headway in the last decade or so. By then the computational resources were widespread enough to make possible large ensembles of long simulations with atmosphere models forced by observed and idealized sea surface temperatures (SSTs). These were used to test hypotheses of oceanic forcing of drought-inducing atmospheric circulation anomalies. Links between North American precipitation variability and the El Niño–Southern Oscillation (ENSO), with, in its El Niño phase, a tendency to increased winter precipitation across southern North America, had begun to be noticed in the 1970s and early 1980s (see Rasmusson and Wallace 1983) and explained in terms of Rossby wave propagation forced by anomalous heat sources over the warm tropical Pacific SST anomalies (Hoskins and Karoly 1981). Trenberth et al. (1988) then applied linear wave theory to link the 1988 drought to the ongoing La Niña event and Palmer and Brankovic (1989) claimed to be able to produce important elements of the same drought within the European Centre for Medium-Range Weather Forecasts (ECMWF) numerical weather prediction model when forced by the observed SSTs.

Explaining a seasonal drought is good progress but it is the multiyear droughts that can wreak the most damage. The Dust Bowl drought lasted about 8 years but was not unique in this regard. Western North America experienced a severe drought from 1998 to 2004 and a severe drought in the early and mid 1950s struck the southwest. Progress in understanding these multiyear droughts had to wait more than a decade. Indeed, as late as 2002, a National Research Council report on abrupt climate change attributed the Dust Bowl drought to atmosphere–land interaction with no role for the oceans (National Research Council 2002). However, in breakthrough studies, Schubert et al. (2004a,b) used large ensembles of atmosphere model simulations forced by

observed SSTs for the post-1930 period to show that the model generated a 1930s drought with both persistent cold tropical Pacific and warm tropical North Atlantic SST anomalies being the drivers. Following up, Seager et al. (2005) and Herweijer et al. (2006) presented SST-forced atmosphere model simulations for the entire post-1856 period of instrumental SST observations and showed that the three observed nineteenth-century droughts, the Dust Bowl, and the 1950s drought were all simulated by the model and argued that persistent La Niña states in the tropical Pacific Ocean were the essential cause of all. Tropical Pacific and Indian Ocean SST anomalies were also invoked as the cause of the multiyear drought that began after the 1997/98 El Niño (Hoerling and Kumar 2003; Seager 2007). The dynamical mechanisms that link tropical SSTs to drought-inducing circulation anomalies have also been studied and the situation of a cold tropical Pacific and warm tropical North Atlantic appears as ideal for inducing drought (Schubert et al. 2008, 2009).

These studies represented considerable advances in understanding why multiyear droughts occur (even though the causes of the persistent tropical SST anomalies that were the drivers has been barely addressed). However, these studies were in many ways broad brush. Long time series, often time filtered, were used to show that the models produced dry conditions at the correct time but then precipitation, circulation, SSTs, and so on were typically averaged over the whole drought period, perhaps by season, for comparing model and observed droughts. Such averaging will tend to emphasize the SST-forced component, which may be fundamental, but prevents a complete analysis of drought onset, evolution, and termination. As such it might prevent proper identification of non-SST-forced components of the drought due to, for example, random atmospheric variations (weather).

For example, during the 1930s Dust Bowl years, while there was no El Niño, the tropical Pacific SST anomalies were only modestly cool and not consistently so, but a drought extended from the southern plains north to the Canadian Prairies and also toward the Pacific Northwest and U.S. Midwest. (Fye et al. 2003; Cook et al. 2007; Stahle et al. 2007; Bonsal and Regier 2007; Cook et al. 2011a). Atmosphere models forced by observed SSTs do simulate a drought during the 1930s with both cooler than normal tropical Pacific and warmer than normal tropical North Atlantic SST anomalies being responsible. However, the droughts are centered in the U.S. Southwest and not in the central plains, as observed, and are also too weak (Schubert et al. 2004a,b; Seager et al. 2005, 2008; Hoerling et al. 2009). Two hypotheses have been advanced to explain the discrepancy. The first is that

the 1930s drought was amplified and moved northward by human-induced wind erosion and dust aerosol–radiation interactions (Cook et al. 2008, 2009, 2011b), and the other is that, instead, the Dust Bowl drought contained a large component of internal atmospheric variability not linked to SST anomalies (Hoerling et al. 2009). Both groups of authors draw a distinction between the spatial extent and severity of the 1930s Dust Bowl drought and the 1950s U.S. Southwest drought with the latter appearing to be more of a canonical SST-forced drought. Similarly, North America is currently within the third year of a drought that has brought successive summers (2011 and 2012) of intense heat and dry conditions to the central part of the continent, from eastern Mexico to Canada. While La Niña conditions prevailed during both summers, it is not at all clear that they alone were sufficient to cause such abnormal conditions with both modes of internal atmospheric variability and, perhaps, climate change having been invoked to provide a full explanation (Hoerling et al. 2013b, 2014; Seager et al. 2014).

Given this state of affairs it appears appropriate to move beyond invoking a general association of drought in southwestern North America and the plains with, primarily, La Niña and, secondarily, warm tropical North Atlantic SST anomalies to consider the causes of North American droughts in more detail, including assessing the role of processes unrelated to ocean forcing. Of particular interest is the extent to which droughts are influenced or driven by internal atmospheric variability relative to being forced by changes in surface ocean conditions. This is important to the understanding of mechanisms but also has serious implications for predictability of droughts. SST anomalies in the tropical Pacific Ocean can be predicted up to a year in advance and, to the extent that they drive atmospheric circulation anomalies over North America, can be potentially exploited to provide seasonal forecasts of drought onset, evolution, and termination. In contrast, aspects of droughts determined by internal atmospheric variability will be unpredictable beyond the weather prediction time scale.

In addition to the potential of SST variability, internal atmosphere processes, and land–atmosphere interaction to cause droughts, we must also address the possibility that human-induced climate change is now impacting North American hydroclimate and the frequency and character of droughts. Seager et al. (2007) and Seager and Vecchi (2010) have shown that a shift toward a more arid climate in southwestern North America begins in the late twentieth century, although it is likely currently masked by natural variability (Hoerling et al. 2011). Also, Hoerling et al. (2013b) have shown that the heat of the 2011 Texas heat wave and drought was likely aided

by global warming, while it was not clear that the precipitation reduction was outside the range of natural variability. Weiss et al. (2009) have also noted the impact of increasing temperatures on southwestern droughts, implying an emerging form of drought in which a warming trend exacerbates the impacts of precipitation reduction.

These considerations motivate the current review paper to take three tacks:

- What are the relative roles of internal atmospheric variability and oceanic forcing in generating droughts over North America? Is a general association between tropical SST anomalies and North American precipitation enough to explain the intensity, spatial coverage, and timing of historical western North American droughts?
- What does the answer imply about the predictability of droughts? Are the most devastating droughts, the most extensive ones that influence multiple nations and agricultural areas, and both upstream and downstream reaches of large river basins, ever simply the result of oceanic forcing or are they instead an unfortunate mix of SST forcing and internal atmospheric variability?
- Even if we can answer the above question, is the scientific ground upon which we stand shifting? That is, are human-induced climate trends—both warming and changes in precipitation—already impacting the likelihood and severity of western North American droughts?

To attempt to answer these questions we will use observations and a variety of model simulations. This is not a typical review in that most of the material presented will be new but it does seek to provide a broad review, motivated by recent research, of where we stand in terms of understanding the causes and mechanisms of North American droughts and to what extent we can anticipate hydroclimate variability and change and, in particular, droughts in the coming seasons to decades.

This review is being performed under the auspices of the Global Drought Information System (GDIS) which is under the World Climate Research Programme (WCRP) umbrella. Hence we aim to contribute to challenges identified at the July 2012 WCRP meeting, including, under “Provision of skillful future climate information on regional scales,” to “Identify and understand phenomena that offer some degree of intraseasonal to interannual predictability” and “Identify and understand phenomena that offer some degree of decadal predictability.” Further, we aim to contribute to the goal under “Interactions across multiplicity of drivers and feedbacks at the regional scale” to “provide increased

understanding of the interplay across the different drivers, processes and feedbacks that characterize regional climate at different spatial and temporal scales. Consider interactions across greenhouse gas forcings, natural modes of variability, land use changes and feedbacks, aerosols, tropospheric constituents.” Models and data used are described next followed by an analysis in sections 3 through 7 of the roles of the ocean and atmosphere in explaining North American precipitation variability over the past century. Section 8 then focuses on the post-1979 period in the U.S. Conclusions are offered in section 9.

2. Observed data and models used

The observed precipitation is the latest version of the Mitchell and Jones (2005) University of East Anglia (UEA) Climatic Research Unit data at 1° resolution (CRU TS3.1). SST data in the observational analysis come from the Hadley Centre (Kennedy et al. 2011a,b). The soil moisture data come from the Climate Prediction Center (CPC) and are an estimate of 1.6-m depth soil moisture in which a leaky bucket model is driven with observed monthly surface temperature and precipitation and have the spatial resolution of the U.S. Climate Divisions (Huang et al. 1996). Observed geopotential height anomalies are taken from the National Centers for Environmental Prediction (NCEP)–National Center for Atmospheric Research (NCAR) reanalysis (Kistler et al. 2001).

We use three sets of atmosphere model simulations of the type referred to as AMIP (for the Atmospheric Model Intercomparison Project) experiments, which are designed to determine the sensitivity of the atmosphere to, and the extent to which its temporal evolution is constrained by, known boundary forcings. The first two are as follows:

- The first ensemble is used for the analysis of the variance of observed and modeled precipitation histories for 1901–2008. This is a 16 member ensemble of SST-forced atmosphere general circulation model simulations for the 1856–2011 period. The model used was the NCAR Community Climate Model version 3 (CCM3) (Kiehl et al. 1998) run at T42 spectral resolution with 18 vertical levels. The only time-varying forcing was the SST, which was from Kaplan et al. (1998) within the tropical Pacific and the Hadley Centre data elsewhere [see Seager et al. (2005) for more details]. Trace gas concentration were held fixed ($\text{CO}_2 = 355$ ppm, $\text{CH}_4 = 1.71 \times 10^{-6}$ ppm, and $\text{N}_2\text{O} = 0.31 \times 10^{-6}$ ppm, all corresponding to levels around 1990) and the sea ice cover has a repeating climatological seasonal cycle. The ensemble mean of these simulations, therefore, closely isolates the SST-forced variations that are

common to the ensemble members by averaging over the uncorrelated weather variations within the individual ensemble members, which begin from different initial conditions on 1 January 1856. This ensemble is called GOGA for “global ocean global atmosphere.”

- To examine precipitation variability in the absence of SST variability we also use a 1100-yr-long simulation with CCM3 forced by a repeating seasonal cycle of SST. Comparing this simulation with the ensembles with the same model forced by realistic SST variability, we can assess whether ocean variations influence the spread of precipitation and frequency of occurrence of dry events of particular durations. This simulation is called COGA for “climatological ocean global atmosphere.” (Model data generated at Lamont can be accessed, without restriction, for visualization, analysis, and downloading at <http://kage.ldeo.columbia.edu:81/expert/SOURCES/.LDEO/.ClimateGroup/.PROJECTS/>.)
- In addition, to focus on variations, especially of soil moisture, in the post-1979 period we use two global atmospheric models with SST, sea ice, and external radiative forcing specified as monthly time-evolving boundary conditions from January 1979 to December 2012. One model used is the NCAR Community Atmosphere Model version 4 (CAM4) global climate model (Gent et al. 2011), with the simulations performed at a 1° resolution and 26 atmospheric levels, and for which a 20-member ensemble is available. The second global climate model used is the ECMWF Hamburg model version 5 (ECHAM5) (Roeckner et al. 2003), with simulations performed at T159 spectral resolution and 31 atmospheric levels, and for which a 10-member ensemble is available. Each realization differs from another only in the initial atmospheric conditions in January 1979, but uses identical time evolving specified forcings. For both models, monthly varying SSTs and sea ice and the external radiative forcings consisting of greenhouse gases (e.g., CO_2 , CH_4 , NO_2 , O_3 , and CFCs) are specified. The CAM4 runs also specify varying anthropogenic, solar, and volcanic aerosols.

In these two cases the SST histories used to force the model include not only SST variability arising from ocean dynamics (e.g., ENSO) and atmospheric forcing but also the response to natural and anthropogenic radiative forcing. This motivates our fourth ensemble:

- To address possible effects of long-term climate change on U.S. drought variability during 1979–2012, an additional 10-member ensemble of ECHAM5 simulations is performed that uses late-nineteenth-century boundary and external radiative forcings. In these so-called ECHAM5-PI experiments, trace gas forcings are set to climatological 1880 conditions and held fixed

throughout the simulation period. Also, the 1880–2012 linear trend in SSTs is removed from the monthly SST variability. This sets the climatological SSTs to values representative of 1880. The SSTs during 1979–2012 otherwise vary identically to those in the AMIP simulations. Two intercomparisons of these parallel simulations are conducted. One is a simple difference of their mean climates to illustrate the signal of long-term change (LTC). The second is a comparison of each model's interannual variability during 1979–2012 to illustrate how temporal variability of U.S. drought may have been affected by long-term change.

For CAM4, column integrated soil moisture to a depth of 0.5 m is used (although results are mostly insensitive to using different soil moisture depths). For ECHAM5 the total column soil moisture is available for diagnosis. To facilitate comparison of observed and modeled soil moisture, the monthly and annual variations are standardized by each model's climatological variability. When comparing to climate division data, model output data have been interpolated onto the U.S. climate divisions.

3. An estimate of the relative roles of the oceans and atmosphere in generating North American precipitation variability

Various factors have contributed to historical North American precipitation variability on seasonal and longer time scales. These include sensitivity to global sea surface temperature variability, local land surface feedbacks including persistent soil moisture states and land use changes, the effects of internal atmospheric variability such as expressed by prolonged circulation states associated with blocking and storm track shifts, and a sensitivity to global warming resulting from changes in external radiative forcing. It is difficult to quantify the contributions of individual factors from the observational record alone, and ensemble climate simulations become a critical diagnostic tool. In this section, SST-forced and internal atmospheric variability are considered, while the effects of long-term climate change will be considered in section 8. Here we use the 16-member GOGA simulations of CCM3. The ensemble mean provides an estimate of the variations common to all ensemble members due to the SST forcing, while the deviations of individual realizations from the ensemble mean provide an estimate of the effects of internal atmospheric variability. While definitions of drought differ, there is broad agreement that a reduction of precipitation is typically required; hence we begin by analyzing precipitation. To address time scales long enough to be relevant to severe sustained drought, we analyze annual mean precipitation.

Figure 1 shows the variance of observed annual mean precipitation. This is greatest, as expected, where the precipitation is greatest, in the Pacific Northwest and the southeast United States, with some other regions of high variance such as the coastal northeast and the Mexican monsoon region. Also shown is the average of the variances of the individual CCM3 ensemble members. This very roughly captures the observed variances in amplitude and spatial pattern although with too low variance in the southeast United States and the eastern coastal states and excess variance in Mexico. Figure 1 also shows the variance of the model ensemble mean, which, as expected, is everywhere much lower than the total model variance. This SST-forced variance has maxima in Mexico and the south and central plains. Finally, the ratio within the model of the SST-forced to the total variance is also shown. This has maxima in northern Mexico, the south to central plains, and the Gulf States. Here, rather remarkably, up to about 40% of the model total annual mean precipitation variance is caused by SST variations.¹ Everywhere else in North America SST forcing accounts for less than a third of total annual-mean precipitation variance (with the lowest values in central and eastern Canada), indicating that the detailed year-to-year variations of precipitation are heavily influenced by internal atmospheric variability. Sustained drought on longer time scales could nonetheless be appreciably influenced by ocean conditions to the extent that the latter are of low frequency and that North American climate is sensitive to temporally coherent patterns of such oceanic forcing. Similar conclusions were reached based on simulations with a different model by Hoerling and Schubert (2010).

The change in precipitation induced by the long-term change in observed SST, which contains a radiatively forced component, can be isolated by computing the trend of the model ensemble mean. This is also shown in Fig. 1 together with its ratio to the standard deviation averaged across the ensemble members. The long-term change in SSTs has, according to the model, induced

¹ Global warming and rising specific humidity is projected by models to cause an increase in interannual hydroclimate variability (Seager et al. 2012a), so we also examined whether the variance of annual mean *P* changed over time in the model. This was done by comparing model variance over 1956–2012 with that over 1856–1912. The variance of the SST-forced GOGA ensemble mean did increase across southern North America, likely due to the very large ENSO variability in the late twentieth century, but the variance of the ensemble members did not consistently change in either way. This implies that the expected global warming-induced increase in hydroclimate variance is not detectable in these 1856–2012 model simulations.

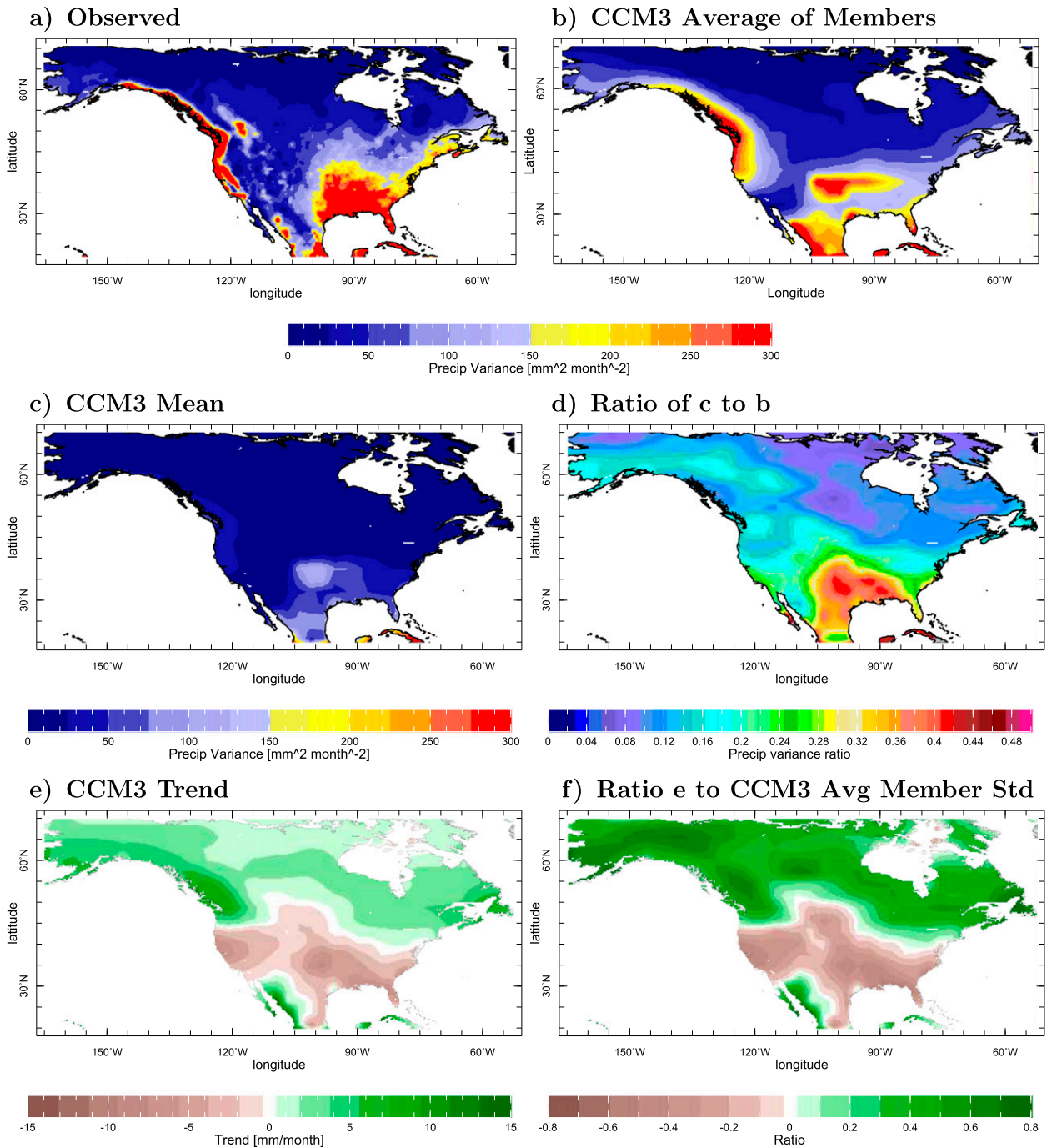


FIG. 1. The variance of (a) annual mean observed precipitation and (b) that simulated by the CCM3 model forced by observed historical SSTs; and (c) the ensemble mean modeled annual mean precipitation, that is, the SST-forced variance and (d) the ratio of the modeled SST-forced to total variance. Variances are in $\text{mm}^2 \text{month}^{-2}$. Also shown are (e) the 1901 to 2009 trend of modeled annual mean precipitation (mm month^{-1}) and (f) the ratio of this to the standard deviation averaged across the model ensemble members (unitless).

a drying across much of the southern half of North America other than western Mexico, and wetting across most of Canada. The amplitude of this relative to the standard deviation of total model precipitation reaches

maxima of about 30% in the southwest and southeast United States and about 50% in northwestern Canada. Based on these model simulations, clearly, while the long-term trend is not negligible, precipitation histories

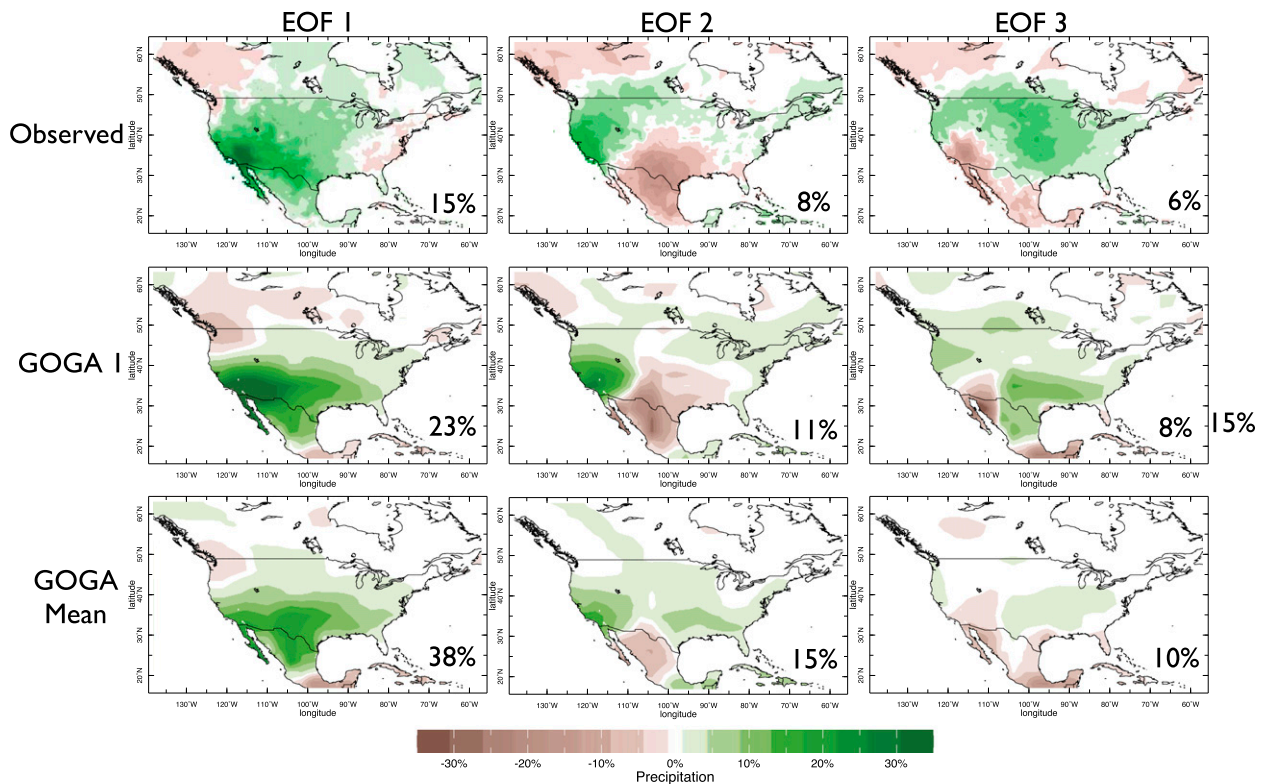


FIG. 2. The first three EOFs of standardized annual mean precipitation anomalies for (top) observations, (middle) a single run of the climate model, and (bottom) the ensemble mean of the model simulations. The percentage of total variance explained is noted on each panel.

to date in subtropical and midlatitude North America will be dominated by natural variability, a point we return to in [section 8](#).

4. Modes of continental-scale precipitation variability

[Cook et al. \(2011a\)](#) conducted an empirical orthogonal function (EOF) analysis of the tree-ring-derived North American Drought Atlas ([Cook et al. 2007](#)), which provides annual estimates of the Palmer drought severity index (PDSI) reflecting surface moisture availability in the spring to summer growing season. They found that the first five modes explained 62% of the variance in the complete record. Of those five modes the first correlated well with tropical Pacific SST variations, while the second appeared to be related to North Pacific atmosphere–ocean variability (not necessarily ocean-forced) and the third to tropical North Atlantic SST variations. The correlations of the PCs to SSTs was strongest in the tropical Pacific Ocean. These results suggested a modest, but important, amount of influence of SSTs on continental-scale modes of hydroclimate variability.

We conduct the same analysis here using annual mean precipitation anomalies. [Figure 2](#) (top row) shows the first three EOFs of the observed detrended (results were essentially the same using the data without detrending) annual standardized precipitation variability (see [Ruff et al. 2012](#)). These explain a large fraction of the contiguous U.S. region variability, although they collectively account for only about 30% of the total variability over all of North America. The first pattern has same sign anomalies across almost all of the United States and Mexico with maximum strength in the U.S. Southwest (where it explains over 30% of the total precipitation variance) and opposite sign anomalies in the Pacific Northwest. The second pattern has a dipole pattern with centers in the Texas–northern Mexico region and the far west where about 20% of the local variability is explained. The third pattern describes an out-of-phase relationship between annual precipitation variability over the monsoon region that encompasses northwest Mexico and the U.S. Southwest and the central Great Plains, reminiscent of a summertime pattern described by [Douglas and Englehart \(1996\)](#) and [Higgins et al. \(1999\)](#).

[Figure 2](#) also shows the same analysis for one simulation of the climate model with global SST forcing and,

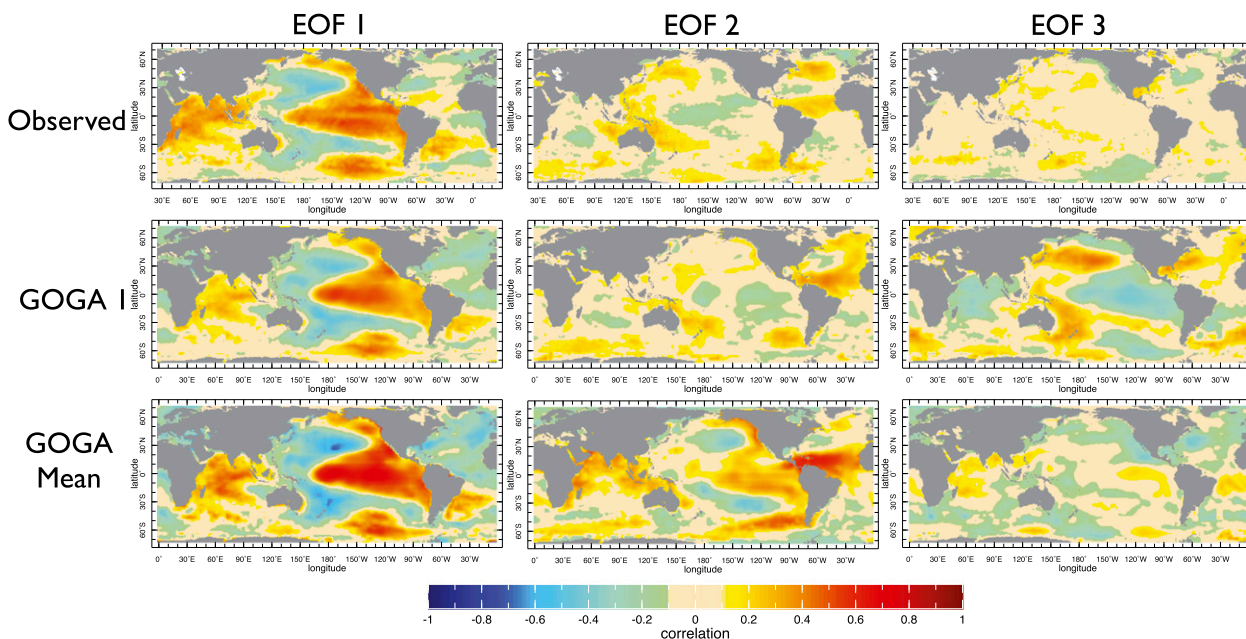


FIG. 3. The correlation of SST anomalies with the PCs associated with the EOF patterns shown in Fig. 2: results for (top) the observations, (middle) a single run of the climate model, and (bottom) the ensemble mean of the model simulations.

in addition, for the ensemble mean of the simulations. The analysis of the single run should be analogous to the analysis of observations since it contains a mix of ocean-forced and internal atmospheric variability and, indeed, the first two EOFs are very similar to those observed and even the third pattern has some similarities. The analysis of the ensemble mean isolates the ocean-forced component in the model. The first ocean-forced pattern is very similar to the observed one, suggesting that this pattern does indeed arise in nature from ocean forcing. The second pattern also contains the north–south dipole along the western coast between Mexico and the United States seen in the observed analysis, but has wrong sign anomalies in the southern plains.

Figure 3 shows the correlation of the principal components of these patterns with global SST anomalies. The first pattern is clearly ENSO, while the second pattern appears to represent a relationship between dryness in Mexico and the southern Great Plains and warm tropical North Atlantic SSTs. This is so in the observations, the model ensemble mean, and the single ensemble member, indicating that these relations between precipitation and tropical Pacific and Atlantic SSTs are quite robust. The SST relations for the third precipitation principal component (PC) are not consistent across observations and models. On the basis of these results for precipitation variability, a cold tropical Pacific/warm tropical North Atlantic emerges as a particularly effective ocean state for forcing drought in the interior southwest and plains, in agreement with Schubert

et al. (2009). A similar link will be shown in section 8 based on analysis of soil moisture variability. As noted in Fig. 2, the first EOFs explain 15% and 23% of the total variance for the observations and the single model run, respectively, and the second modes 8% and 11%. These modest values of the two clearly SST-associated modes are consistent with the results shown in Fig. 1. For the ensemble mean the variances explained by the SST-forced modes are much higher because the internal atmosphere variability is largely, but not entirely, missing due to the averaging across ensemble members.

5. Observed and modeled precipitation variations in the Great Plains and southwest North America over the past century

From what has been presented so far we would expect that the atmosphere model forced by historical observed SSTs would, by simulating the ocean-forced component, capture some, but by no means all, of the observed history of precipitation over western and central regions of North America. Figure 4 shows comparisons of modeled and observed precipitation for both the Great Plains region (here defined as 30°–50°N, 110°–90°W, land areas only) and southwest North America (SWNA) (here defined as 25°–40°N, 125°–95°W, land areas only). The model ensemble mean represents the SST-forced component, and the shading around it ± 2 standard deviations of the ensemble spread and shows whether the observed precipitation anomalies ever fall outside the

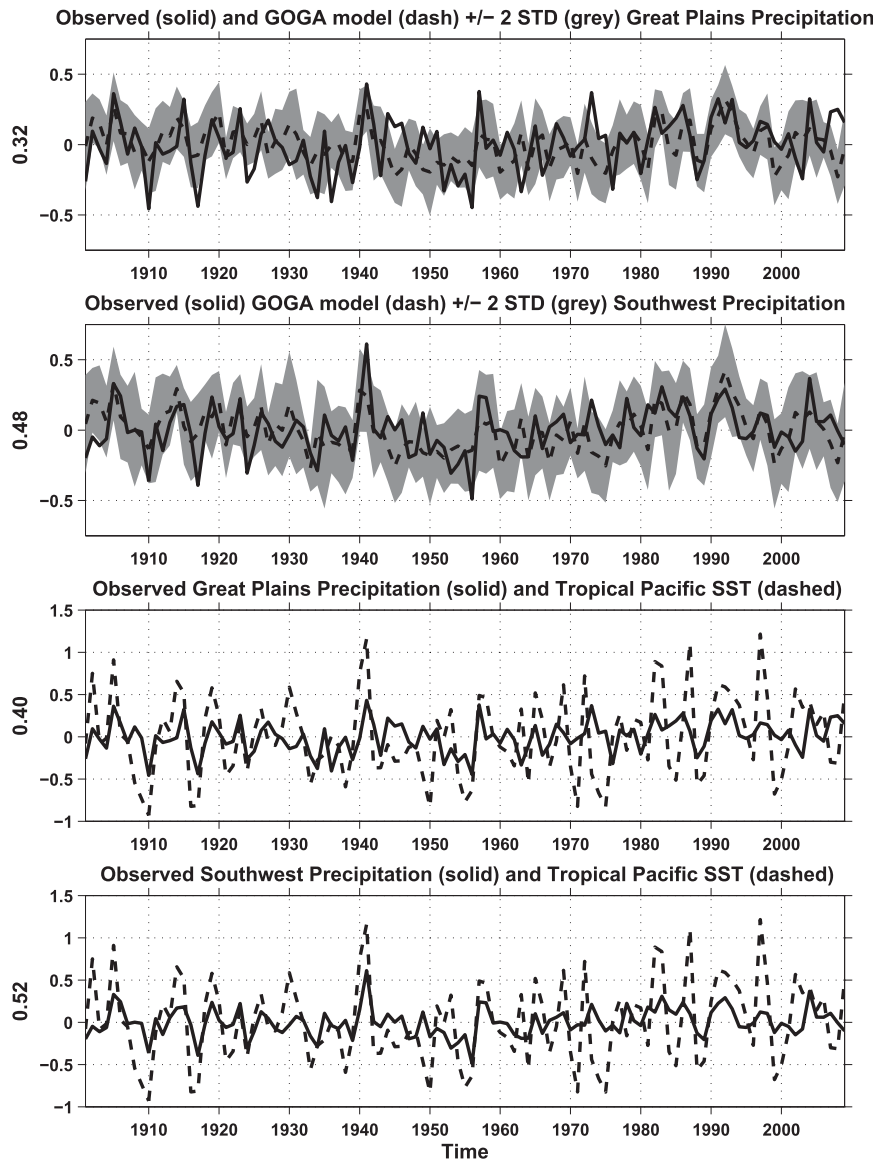


FIG. 4. The observed (solid line) and modeled (ensemble mean as dashed line with two standard deviation ensemble spread shown by shading) history of annual mean precipitation (mm day^{-1}) for (top) the Great Plains and (middle top) southwest North America. Also shown is the observed annual mean precipitation for (middle bottom) the Great Plains and (bottom) southwest North America, together with the tropical Pacific SST history (K).

range of the model ensemble. The best model reproduction of the observed history is in SWNA where about a quarter of the observed variance of annual means can be explained in terms of SST forcing. Individual wet and dry years are quite well simulated, as well as the longer-term multiyear to decadal variability. The model–observations comparison for the Great Plains is not quite so impressive but, given the similarity of the observed SWNA and plains records, many of the same points hold true. The role of Pacific decadal variability is clear in the shift in the mid-1970s in both

regions from overall drier conditions since the early 1940s to wetter conditions until the 1997/98 El Niño (see Huang et al. 2005).

The lower two panels of Fig. 4 explain much of why the model is capable of reproducing important features of Great Plains and SWNA precipitation history by plotting together the observed precipitation history with that of SST averaged over $5^{\circ}\text{S}–5^{\circ}\text{N}$, $180^{\circ}–90^{\circ}\text{W}$ [the tropical Pacific (TP) index]. The TP index correlates with plains precipitation at 0.40 and with SWNA precipitation at 0.52. The 1980s and 1990s were a time of

warm El Niño–like conditions [as noted first by Zhang et al. (1997)], whereas the dry conditions between the 1930s and 1950s correspond to overall cooler La Niña–like conditions, with the exception of the early 1940s El Niño, which caused striking wet conditions in both the plains and SWNA that are well reproduced by the model. In both regions, most dry years were associated with cold TP SSTs but there are exceptions to this (2003 is one) and there are also cold tropical Pacific years that were not dry years. The model precipitation–tropical Pacific SST correspondence is good (see also Schubert et al. 2008), given that we know that internal atmospheric variability accounts for a larger proportion of precipitation variability than does ocean forcing and, even for the latter, the tropical Atlantic SSTs play an important role too (Enfield et al. 2001; McCabe et al. 2004; Schubert et al. 2008; Kushnir et al. 2010; Nigam et al. 2011). It is obvious that the tropical Pacific Ocean is a major orchestrator of North American hydroclimate.

Comparisons of modeled and simulated precipitation that extend back a century or more are still relatively rare but the ones that do exist confirm what would be expected on the basis of Fig. 1. For example, SST-forced models can reproduce precipitation history across Mexico with some fidelity (Seager et al. 2009b) but the skill in the southeast United States is decidedly low and confined to the winter season (Seager et al. 2009a), and nonexistent in the northeast United States (Seager et al. 2012b).

6. Hydroclimate variability owing to internal atmospheric variability

While there seems to be no doubt that variations in tropical Pacific SSTs can force drought conditions over western and central North America, it is also clear that the actual drought history cannot be explained entirely in this way. Although for the special case of the Dust Bowl land surface degradation and dust storms likely played an important role in shaping the drought (Cook et al. 2008, 2009, 2011b), more general is the likelihood that droughts were initiated, evolved, and terminated by some mix of SST-forced circulation anomalies and internal atmospheric variability (e.g., Hoerling et al. 2009). To assess this we first address a simpler question: what would hydroclimate and drought variability be like in the absence of any ocean forcing of variability? Histograms of 1-, 3-, 5-, and 7-yr mean precipitation anomalies, shown in Fig. 5, were computed for the southwest North America domain with both the entire COGA simulation and 1100 years sampled from the GOGA ensemble members. First of all, the GOGA distribution is quite similar to that evaluated from the Global Precipitation

Climatology Centre (GPCC) observations (not shown). The model comparison shows that, for all durations of precipitation anomalies, the GOGA distribution is wider than the COGA one. Indeed, for the 5- and 7-yr duration events, the difference is between infrequent events in GOGA and almost nonexistent events in COGA. The pairs of distributions are, however, not different at the 5% level according to a two-sample Kolmogorov–Smirnov test. Nonetheless, these results do suggest that, within this model, SST variability notably increases the variance of precipitation, making persistent droughts more likely than they would be based on atmospheric processes alone. Qualitatively, the same result holds for the Great Plains domain. Presumably these results are contingent on the nature of actual observed SST variability, which does contain periods of persistence in both Pacific and Atlantic Oceans, which can introduce persistence in precipitation anomalies over North America.

7. Simulation of two historical droughts and one mystery event

So, given these general measures of temporal and spatial variability of annual mean precipitation over North America, can multiyear droughts be explained in terms of ocean forcing? Or, to rephrase the question, does the existence of ocean conditions conducive to drought guarantee that a drought will, in fact, occur? To assess this we focus on two historical multiyear drought periods: 1952–56, which is the core of a decade-long period considered the drought of record for portions of the southern Great Plains (e.g., Hoerling et al. 2013b), and 1999–2002, which constitutes the first several years of a decade-long drought epoch, especially affecting southwest North America, that began after the 1997/98 El Niño (Hoerling and Kumar 2003; Lau et al. 2006; Seager 2007). Figure 6 shows the observed anomalies of near-global SST, 200-hPa heights (from the NCEP–NCAR reanalysis), and North American precipitation averaged over these events, relative to a 1949–2009 climatology. Generally warm SST anomalies and positive heights in the latter period are evidence of global warming. However, cool tropical Pacific anomalies are evident in both periods, as well as relatively low geopotential heights over the tropics. In the extratropics of the Northern Hemisphere there are wide areas of high pressure affecting North America in both cases—an expected response to cool tropical Pacific SST anomalies (e.g., Seager et al. 2003; Lu et al. 2008; L’Heureux and Thompson 2006). [The Southern Hemisphere height anomalies are probably dominated by trends caused, primarily, by ozone depletion (Cai and Cowan 2007; Son

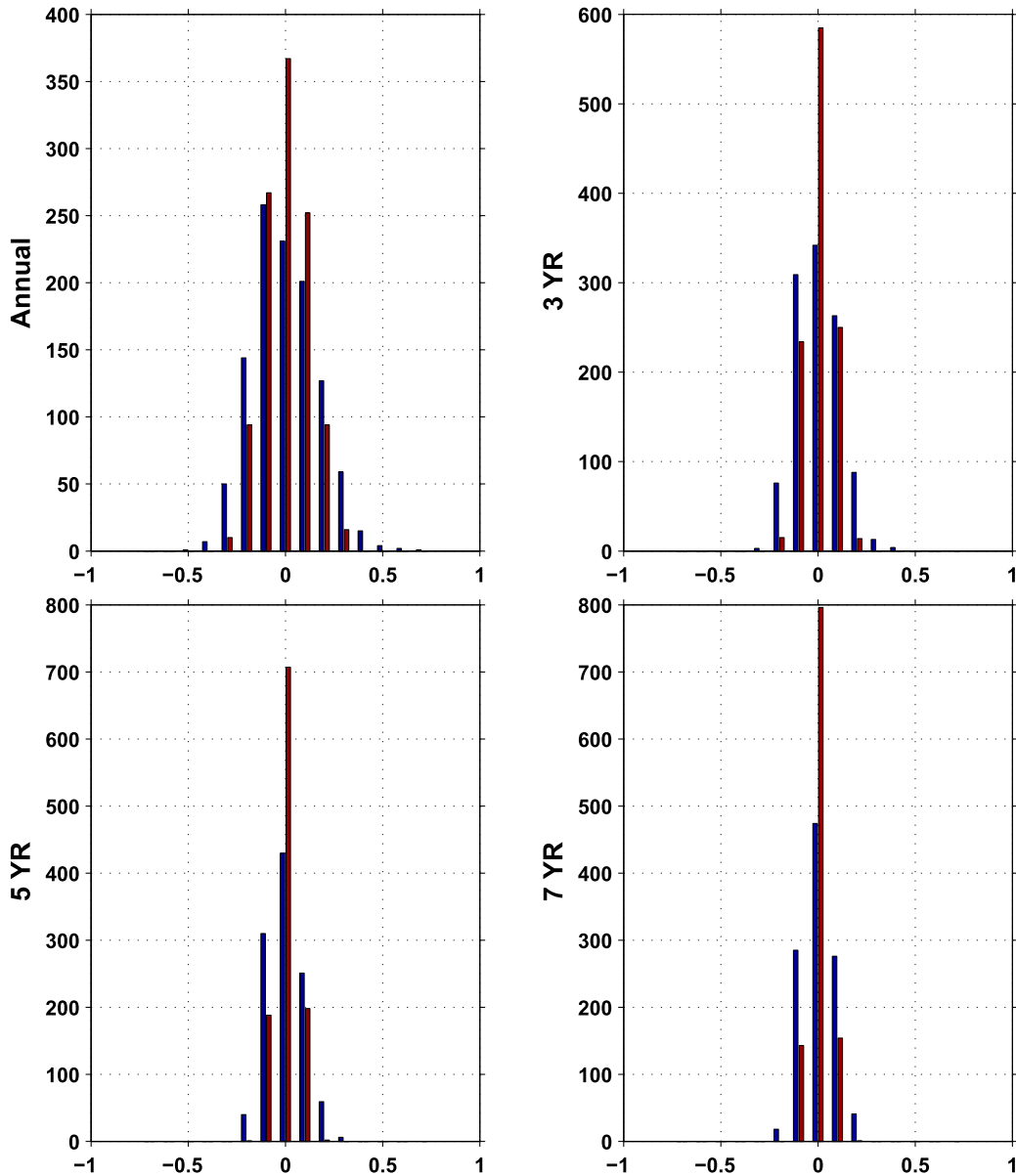


FIG. 5. Histograms of 1-yr, 3-yr, 5-yr, and 7-yr mean precipitation anomalies (mm day^{-1}) across southwest North America computed from simulations of an atmosphere model forced by observed time-varying SSTs (GOGA) and from the same model forced by a repeating seasonal SST climatology (COGA). In the COGA simulation variability arises from atmospheric processes alone, which leads to weaker amplitude variability, and fewer persistent anomalies, than in the case with ocean variability.

et al. 2009; Polvani et al. 2011) and do not clearly show the La Niña pattern.] The observed drought in 1952–56 was striking in its severity, encompassing the U.S. Southwest, Great Plains, Southeast, and Midwest. The 1999–2002 drought was modest by comparison and more focused in the entire west of North America including Canada.

Figure 7 shows the model simulation of these two droughts. Again the general tendency to rising heights

associated with the warming oceans is evident, but the relatively low tropical heights forced by the cool SSTs are evident. The model also produces modest ridges in northern midlatitudes, including over North America, as in the observations. The extratropical ridges are more clear in the turn-of-the-century drought, also as in observations. The model does a credible job of simulating the spatial extent of each drought, although the 1950s one is clearly weaker than observed. The comparisons of

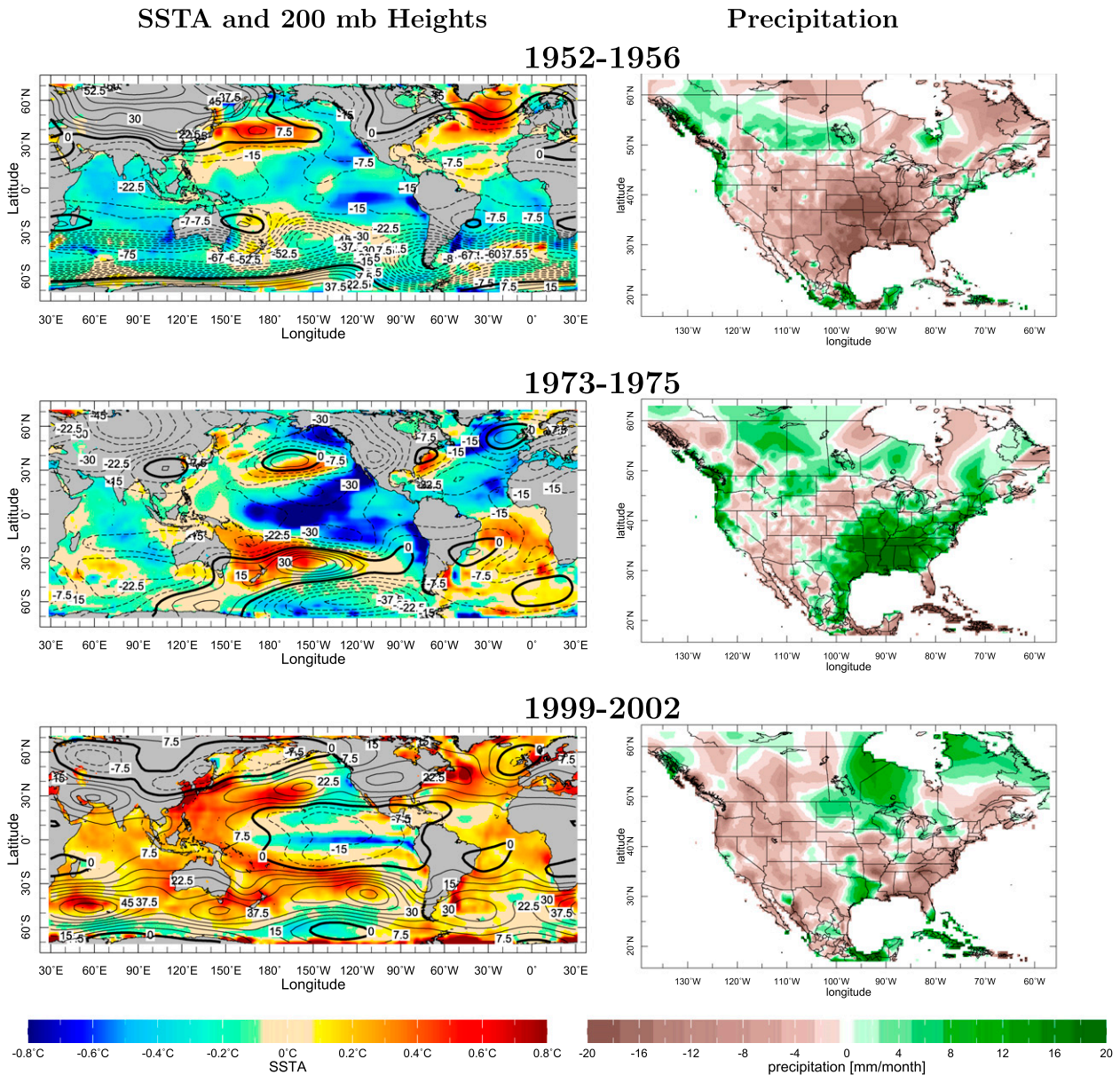


FIG. 6. The observed SST (K), 200-hPa geopotential height (m), and North American precipitation anomalies (mm month^{-1}) during droughts in 1953–56 and 1999–2002 and the 1973–75 event.

heights and precipitation for both droughts are consistent with ocean forcing generating the droughts but with a large additional role for internal atmosphere variability in determining the details.

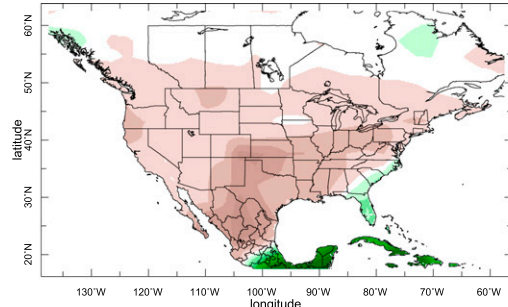
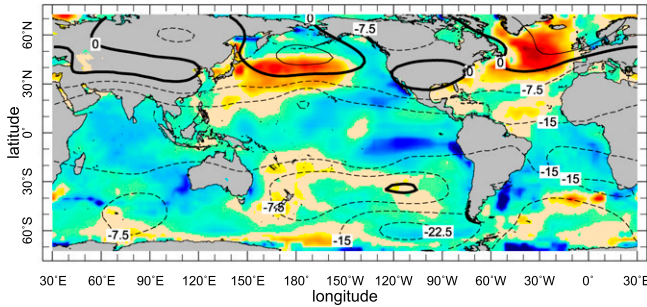
The middle panels of Figs. 6 and 7 show the case of the mystery event of 1973–75. This was a period of an extended La Niña between the 1972/73 and 1976/77 El Niño events. The low tropical heights expected are clearly seen as well as a well-developed wave train extending into the Southern Hemisphere, but the Northern Hemisphere height anomalies show a circulation pattern distinctly unlike La Niña. Consistent with the

circulation anomalies, there was little evidence of the normal La Niña-induced drying with just a patch of reduced precipitation in the southwest. The model simulations (Fig. 7), however, show, as expected, a classical La Niña-induced pattern of circulation anomalies including a (relative) ridge across the North Pacific and North America and, consistently, widespread precipitation reduction across North America (see also Fig. 4). The model therefore suggests that the early 1970s should have been a multiyear drought much like that in the 1950s and at the turn of the century—not surprising given the strong La Niña—but apparently other

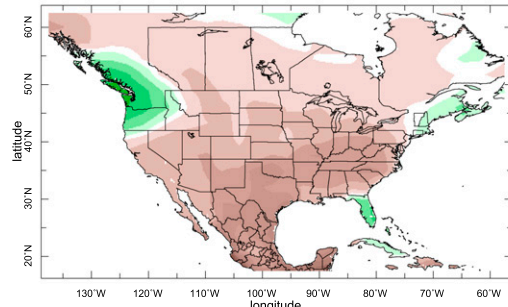
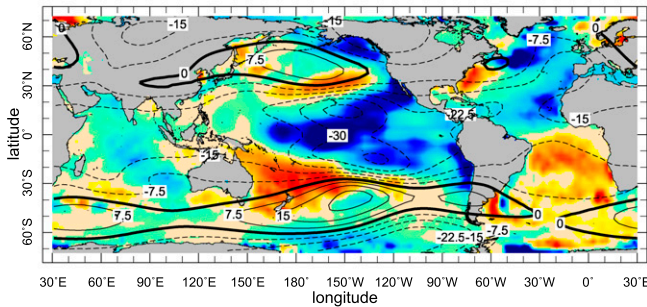
SSTA and 200 mb Heights

Precipitation

1952-1956



1973-1975



1999-2002

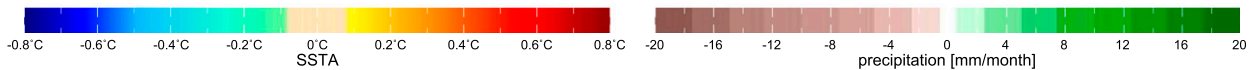
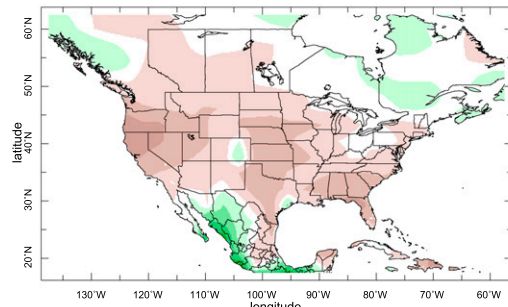
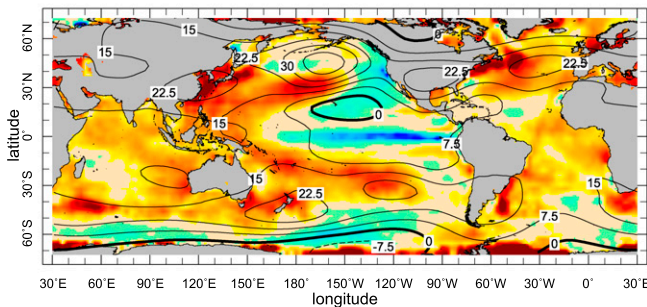


FIG. 7. As in Fig. 6, but for the model simulation.

sources of atmospheric variability were, for this event, able to overcome the influence of the tropical Pacific Ocean. The model simulations presented by Schubert et al. (2004a) and Lau et al. (2006) contain a similar discrepancy. The cold tropical Atlantic and Indian Ocean SSTs may have played a role with this influence being missed or too weak in the models [see Lau et al. (2006) for a discussion of the relative influences of equatorial east Pacific and Indo-west Pacific SST anomalies]. However, it is also likely that random internal atmospheric variability could have overwhelmed ocean nudging toward dry conditions in 1973–75, consistent with the analysis of the probability distributions

of SST-forced ensembles to be presented in section 8. In support of this idea, the time series of model ensemble mean and spread in Fig. 4 show that some ensemble members produced wet conditions during the 1973–75 period.

The better model–observed geopotential height agreement for the turn-of-the-century drought than for the 1950s drought might be because of problems with the data in the presatellite era and, indeed, the height anomalies in the Twentieth-Century Reanalysis (Compo et al. 2011), the only other reanalysis to cover the 1950s, are different (not shown). For the remainder of the paper we focus on the drought record for the well-

Soil Moisture

EOF 1 21%

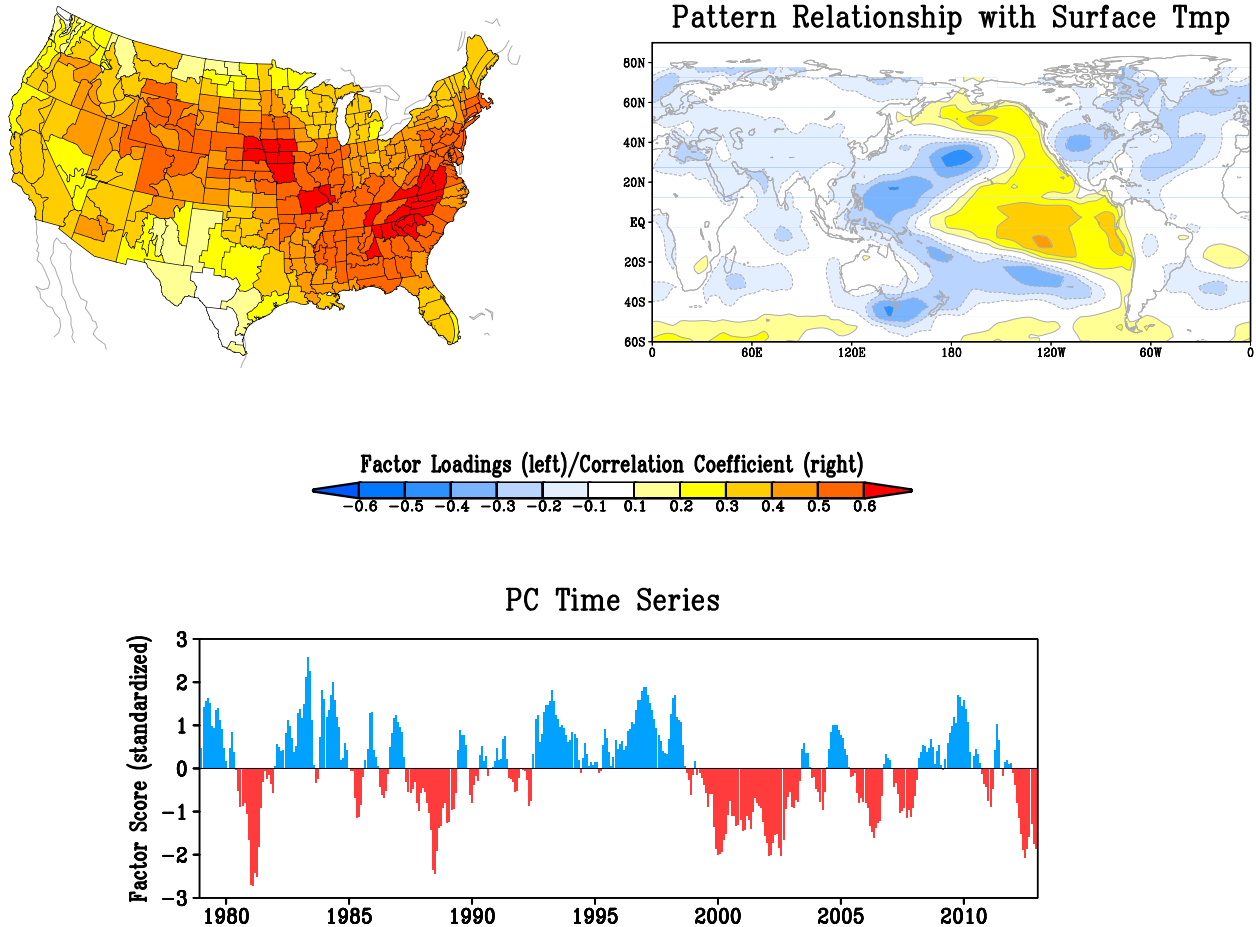


FIG. 8. The (top left) spatial pattern and (bottom) PC time series of the first empirical orthogonal function (EOF1) of monthly soil moisture. Analysis is of the correlation matrix of 408 monthly samples of Climate Prediction Center estimated soil moisture during January 1979–December 2012. U.S. map plots the local correlation of monthly soil moisture with the PC time series. (top right) Monthly correlation of the PC time series with observed surface temperatures during 1979–2012.

observed period since 1979 to develop a closer look at recent and ongoing events.

8. U.S. drought variability since 1979

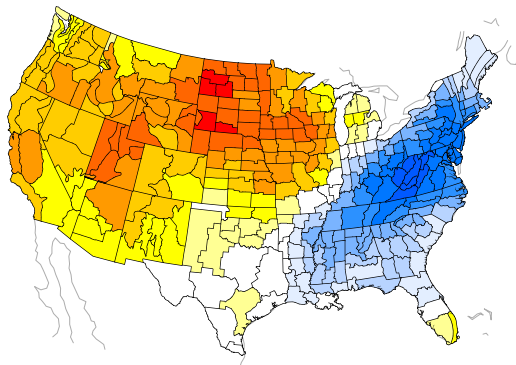
The post-1979 period corresponds to a well-observed period after the introduction of satellite data in the 1970s. This is also a period of substantial global warming and contains several severe drought events over the contiguous United States. We conduct an analysis of soil moisture variability during this last 34-yr period in order to assess the integrated effects of temperature and precipitation on drought. Availability of quality soil moisture data means that this analysis is restricted to the contiguous United States.

a. Leading patterns of U.S. soil moisture variability

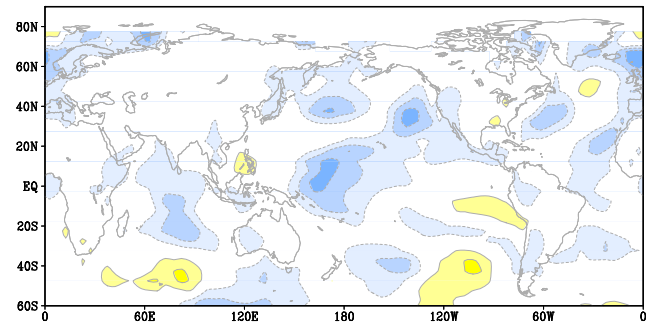
We begin, as for precipitation, by determining the leading patterns of soil moisture variability using an EOF analysis. The principal component time series associated with the spatial structures are then regressed with SSTs to identify connections to ocean variability. Figures 8, 9, and 10 show the first three EOFs of monthly soil moisture variability, which together explain about 46% of the total monthly contiguous U.S. soil moisture variability. (This percent of variance explained is higher than that found for the precipitation analysis in Fig. 2. This is probably because soil moisture integrates precipitation minus surface evapotranspiration in time, effectively averaging over the highest

Soil Moisture

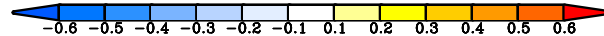
EOF 2 15%



Pattern Relationship with Surface Tmp



Factor Loadings (left)/Correlation Coefficient (right)



PC Time Series

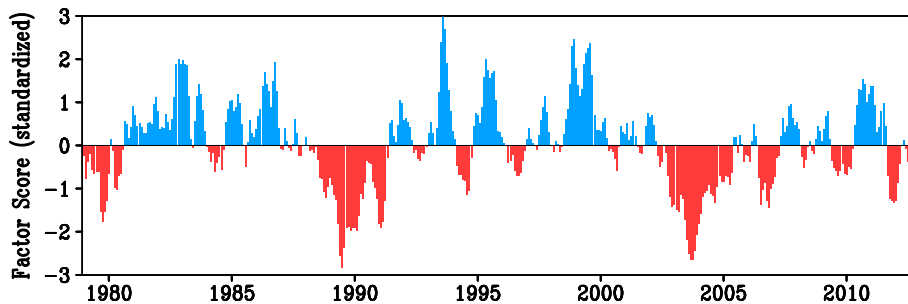


FIG. 9. As in Fig. 8, but for the second EOF.

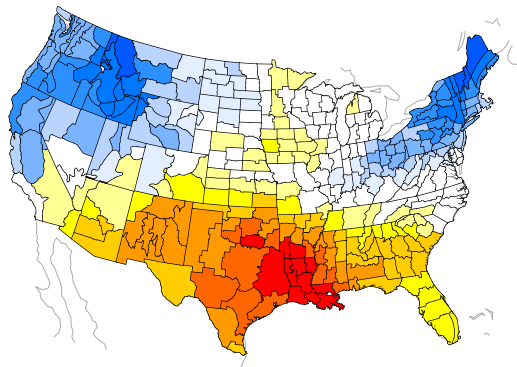
frequency precipitation variations generated by internal atmospheric variability.) The leading structure describes a nationwide pattern of like-signed anomalies with maxima over the central Great Plains and the Ohio and the lower Mississippi River valleys (Fig. 8). Its PC time series suggests that national-scale drought conditions occurred only sporadically and briefly in the 1980s and 1990s, whereas an abrupt change from moist to dry conditions in the late 1990s led to a predominately dry state during the last decade. The monthly time variability of this pattern is significantly correlated with Pacific Ocean variability resembling ENSO and Pacific decadal variability (Fig. 8, top right), a relationship also found between the leading North American pattern of precipitation variability and SSTs (see Fig. 3). Cold phases of an ENSO-like pattern are correlated with low U.S. soil moisture and also with warm U.S. surface

temperatures. The drier conditions since the late 1990s are associated with a cooler tropical Pacific Ocean. An additional, though weaker, SST correlation occurs between warm phases of the North Atlantic SSTs and dry/warm states of U.S. monthly climate. These Pacific and Atlantic SST correlations, though each explaining only a modest fraction of the monthly variance of U.S. soil moisture associated with EOF1, are consistent with an interpretation of oceanic forcing as supported by empirical analysis using century-long datasets (e.g., McCabe et al. 2004) and climate model simulation studies (e.g., Schubert et al. 2009; Findell and Delworth 2010).

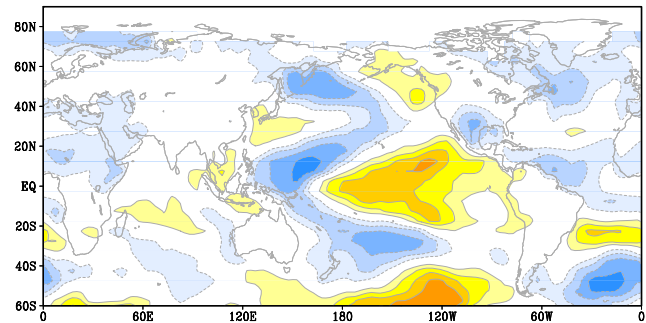
The second EOF (Fig. 9) explains large variance in soil moisture over the northern Great Plains–upper Midwest region and also over the eastern United States. The dipole structure here might well be an artifact of the spatial orthogonality requirement within the analysis

Soil Moisture

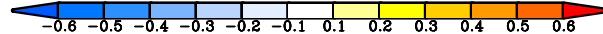
EOF 3 11%



Pattern Relationship with Surface Tmp



Factor Loadings (left)/Correlation Coefficient (right)



PC Time Series

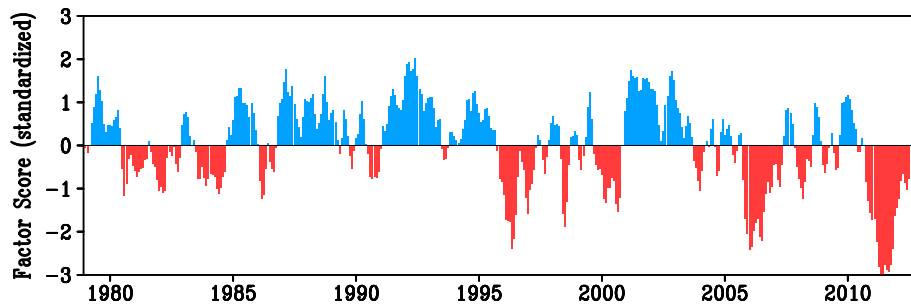


FIG. 10. As in Fig. 8, but for the third EOF.

rather than a genuine anticorrelation between these two regions (see below). This pattern's PC time series captures variability associated with a particularly dominant northern plains drought event that occurred during the 1988–90 period. The negative values of the PC time series for 2003–05 primarily describe an unusually wet period that occurred over the eastern United States, as revealed by inspection of annual rainfall anomaly maps, rather than a severe drought epoch in the northern plains (not shown). The principal component time series of this second EOF exhibits little significant or spatially coherent SST relationship (Fig. 9, top right). There is a hint that cold states of the central equatorial Pacific may be linked with the dry soil moisture conditions in the northern United States. This correlation owes principally to the fact that the late-1980s northern U.S. drought occurred during a strong La Niña event, an

association that was initially conjectured to denote a cause-and-effect linkage (e.g., Trenberth et al. 1988; Palmer and Brankovic 1989) but was refuted by subsequent studies (Lyon and Dole 1995; Liu et al. 1998; Chen and Newman 1998; Bates et al. 2001). Supporting the notion that La Niña is not a particularly effective driver of northern Great Plains drought, precipitation over this region has been above average during the several La Niña events that occurred since 1988, including during 1999/2000, 2007/08, and 2010/11.

Finally, shown in Fig. 10 is the third EOF structure of monthly soil moisture variability. This describes locally strong variance over the southern Great Plains, the Pacific Northwest, and the U.S. Northeast—a pattern similar to the second EOF of annual precipitation (see Fig. 2). A principal drought event described by this pattern occurred during 2011 centered over Texas. The PC

time series of EOF3 is correlated with a tropical Pacific SST pattern resembling ENSO, with cold ENSO phases related to southern plains low soil moisture. Such a relationship is indicative of a forcing–response relationship, as suggested by modeling studies linking the prolonged cold state of the tropical Pacific during the late 1940s–mid-1950s to protracted severe southern plains drought (e.g., Seager et al. 2005; Hoerling et al. 2009) and also linking the strong La Niña event of 2011 with the southern plains drought (Hoerling et al. 2013b, 2014; Seager et al. 2014). We also note that dry southern plains conditions are weakly correlated with warm states of the tropical North Atlantic, consistent with a similar relationship between the second EOF of precipitation and Atlantic SSTs during the longer historical record (see Fig. 3).

We would not expect the EOF analyses of soil moisture here, and of SSTs in section 4, to completely agree since soil moisture does not have a simple relationship to precipitation and the periods covered are also different. However it is clear that the first EOFs do actually agree on the tropical Pacific SST influence on widespread continental-scale dry anomalies and that the second precipitation EOF and third soil moisture EOF are related and point out the influence of a cold tropical Pacific/warm North Atlantic SST pattern on dryness in the northern Mexico–southern Great Plains region and wetness in the Pacific Northwest.

b. Diagnosis of individual extreme drought events during 1979–2012

Here two particular aspects of U.S. drought variability are diagnosed. One seeks to explain occurrences of individual severe events during 1979–2012, and we explore the extent to which the timing and location of these can be reconciled with climate signals forced by varying global sea surface temperatures, sea ice, and atmospheric trace gases. The question addresses potential predictability of such discrete drought events, as inferred from a diagnosis of the factors that may have caused them. A second seeks to explain the broader national-scale context of drought variability, and we explore the temporal evolution of drought coverage averaged over the entire contiguous United States during 1979–2012. The question addressed is the role of longer-term climate variability and change in U.S. drought variability as a whole.

Four of the principal U.S. droughts since 1979 are identified from the PC time series of soil moisture variability, and the spatial maps of their soil moisture departures are presented in Fig. 11 (left side). For simplicity, annually averaged soil moisture departures are presented and, while realistically describing the spatial coverage of drought associated with each case, these

analyses do not necessarily capture the peak intensity of drought during each event. For instance, the 1988 and 2012 events have been characterized as flash droughts having in both cases witnessed sudden onset in late spring followed by a rapid intensification during summer (e.g., Chen and Newman 1998; Hoerling et al. 2014). In contrast, the 2000 and 2011 droughts spanned multiple seasons (Hoerling and Kumar 2003; Hoerling et al. 2013b; Seager et al. 2014) and were comparatively more long-lived events.

Before diagnosing the role of forcing in these four events, we assess the typical spatial scale of soil moisture variations associated with droughts over these geographical regions. Figure 11 (right panels) shows the result of a one-point correlation between monthly soil moisture variability at each climate division with the variability of a soil moisture index that samples each of the four regions having severe drought events (outlined by dark contours on the maps in the left column of Fig. 11). Soil moisture variations over these drought-prone areas have a distinct regional scale that is mostly uncorrelated with soil moisture variations over the rest of the United States. As such, dipole patterns of opposite-signed soil moisture extremes indicated by the EOF analysis appear not to be a general condition. In particular, the empirical patterns of U.S. soil moisture variability identified by EOF2 (Fig. 9) and EOF3 (Fig. 10) should not be interpreted as preferred physical patterns of soil moisture variability over the United States as a whole. On the other hand, the one-point correlation results do suggest that a simple index of contiguous U.S. area-averaged soil moisture would typically be a meaningful indicator of regional drought events, consistent with inferences drawn from the leading EOF pattern of soil moisture variability (Fig. 8).

The question of whether particular oceanic and external radiative forcings may have exerted a substantial influence on these four drought events is addressed using the 40-member ensemble of two different models run over the period 1979–2012. Figure 12 presents two particular aspects of the simulated sensitivity. The spatial plots (left) present annual mean, ensemble-averaged soil moisture departures for each of the four cases, whereas the probability distributions (PDFs, right) summarize the 40-member range of simulated soil moisture departures. These have been spatially averaged over the drought regions outlined in the left panels.

The climate simulations indicate a general absence of forced drying over the northern Great Plains–Midwest drought area during 1988 (Fig. 12, top). Consistent with prior climate model studies of the 1988 period, these new simulations indicate that any mean forced response was either negligible or not detectable and the 1988 drought resulted largely from internal atmospheric

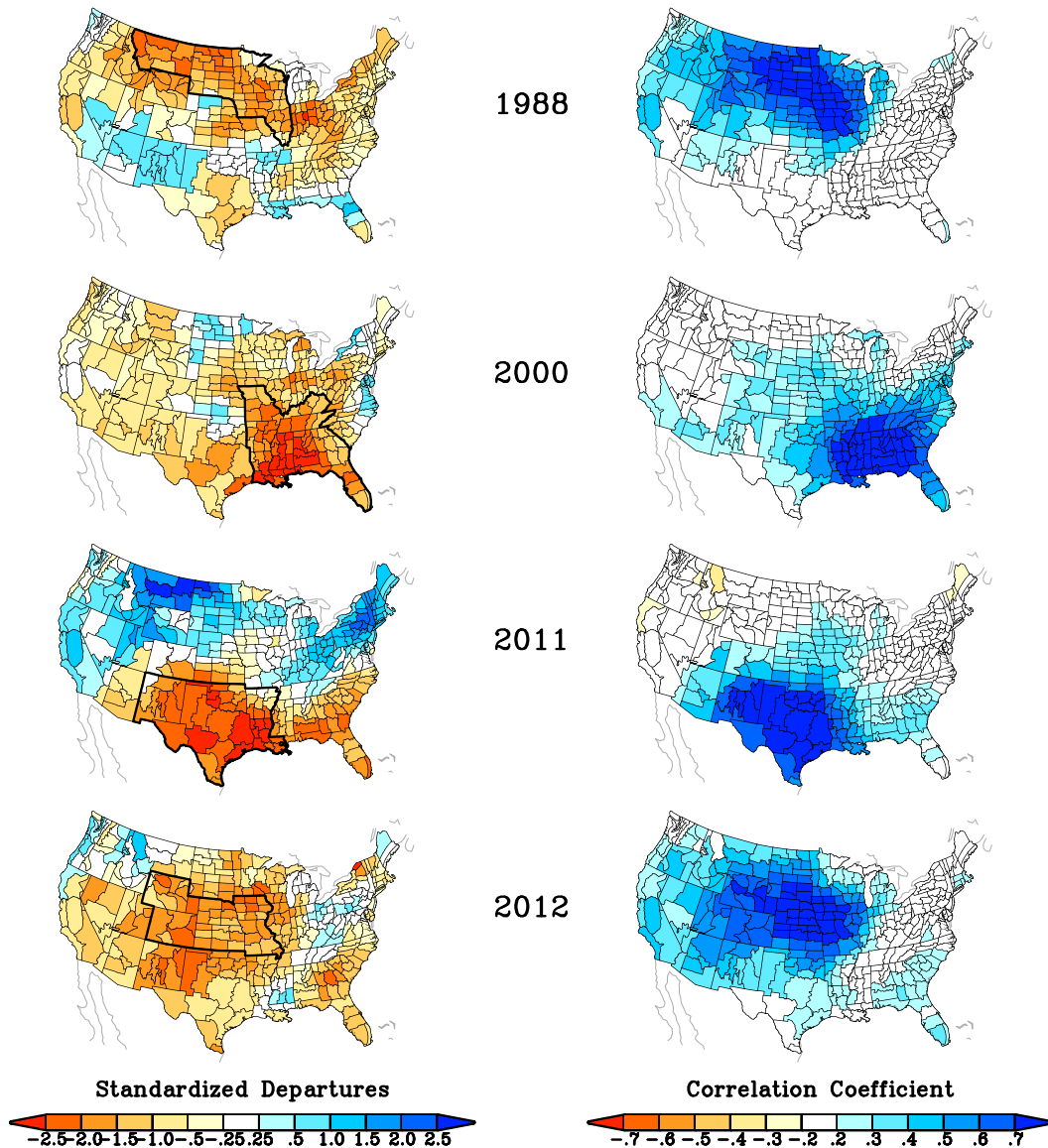


FIG. 11. (left) Estimate of annually averaged soil moisture departures (mm) for (top) 1988, (second row) 2000, (third row) 2011, and (bottom) 2012. Outline highlights core region for each drought event. One point correlation maps (right) of the monthly soil moisture variability at all 344 U.S. climate divisions with the 1979–2012 time series of soil moisture averaged for each of the four drought regions.

variability. By contrast, the model simulations indicate that each of the subsequent drought events had substantial forced components. Signals of dry soil moisture occur over each of the regions that experienced severe drought in 2000, 2011, and 2012 (Fig. 12, bottom three panels) with magnitudes of about 1–1.5 standardized departures. The spatial patterns of those signals are quite similar to one another—more so than the observed patterns of soil moisture anomalies for these events. The evidence from these simulations is nonetheless strong that particular conditions of ocean states and/or

external radiative forcing during those years significantly increased probabilities for severe drought to occur over the areas that indeed experienced severe drought.

Several lines of evidence indicate that the forced signal of dryness and the associated increase in severe drought risk in these three years was mostly due to natural oceanic variability. Consider first the SST correlations with the PC time series of soil moisture EOF1 and EOF3 (see Figs. 8 and 10); both indicate significant tropical Pacific SST links to soil moisture variability over portions of the Great Plains and southern United States,

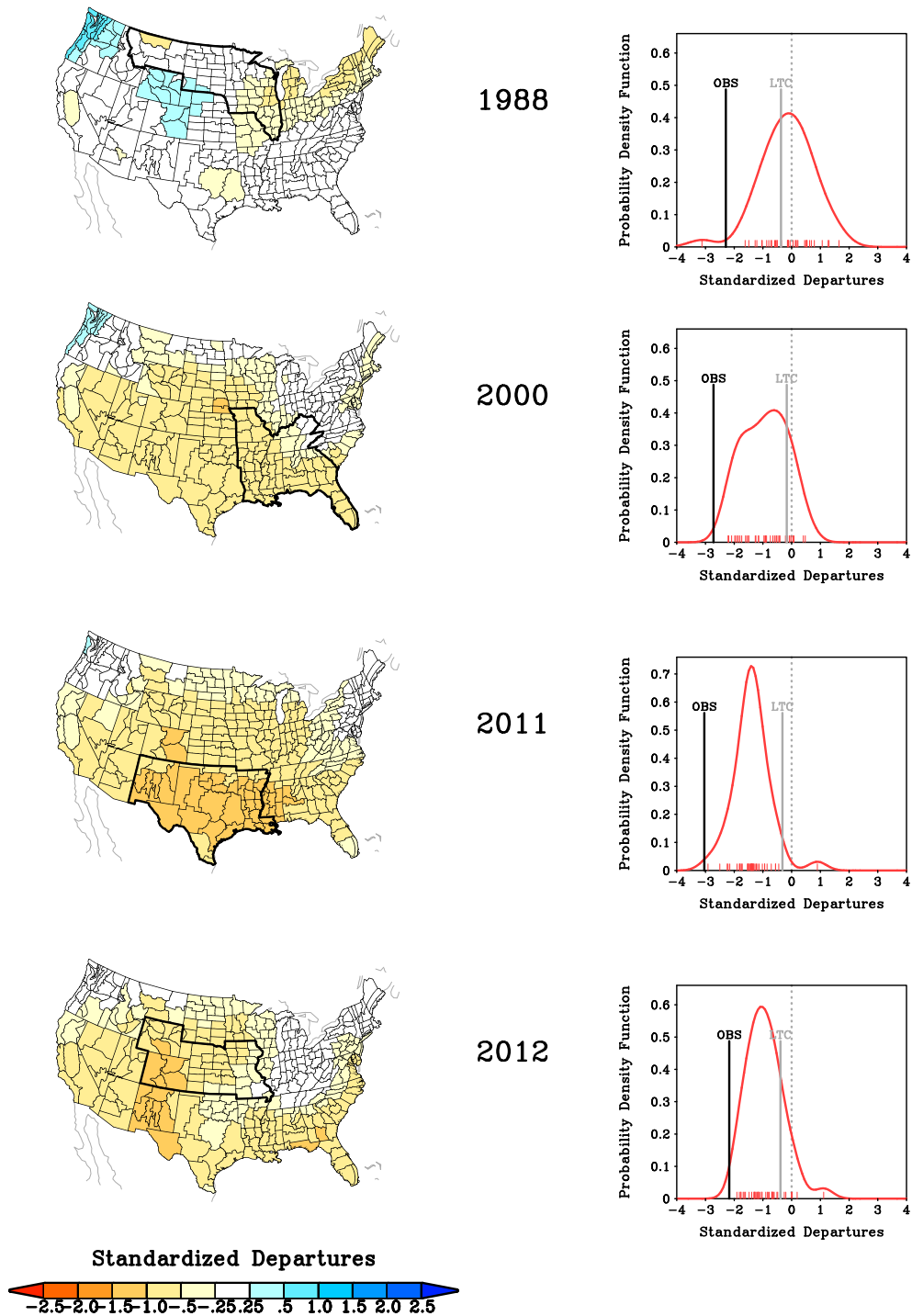


FIG. 12. Simulated annually averaged soil moisture departures (mm, left) for (top) 1988, (second row) 2000, (third row) 2011, and (bottom) 2012 based on a 40-member ensemble mean of models forced by the observed SST, sea, ice, and atmospheric trace gas variability. Outline highlights core region for each observed drought event. Soil moisture probability distribution functions of the 40 separate climate simulations (red), with the observed (black bar) and estimate long-term climate change (LTC) (gray bar, see text for further details) departures. Red tick marks at the bottom denote the simulated values for each ensemble member.

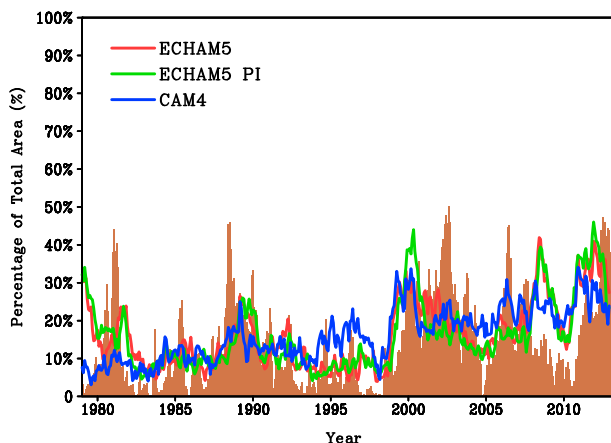


FIG. 13. Monthly time series of the percent area of the contiguous United States with estimate soil moisture anomalies less than one standard deviation (brown); same analysis based on the ensemble averaged of fully forced CAM4 simulations (blue), fully forced ECHAM5 simulations (red); and a parallel ensemble of ECHAM5 (ECHAM5-PI) simulations in which trace gas forcings are set to climatological 1880 conditions and the 1880–2012 linear trend in SSTs is removed from the monthly SST variability.

on interannual and longer time scales. Results in sections 4, 5, and 8a and from prior modeling studies reveal that drought is more likely over these regions when tropical Pacific SSTs are cold (e.g., Seager et al. 2005; Schubert et al. 2009). The drought years 2000 and 2011 indeed occurred in concert with strong La Niña events. The results of the new climate simulations presented here, when taken together with such prior modeling and empirical evidence, therefore support the argument that the droughts resulted in part from strong La Niña-related forcing. By contrast, the 2012 ocean conditions were only modestly cold in the tropical Pacific. However, tropical North Atlantic conditions were especially warm that year (not shown, they were also warm during 2000 and 2011). The simulated 2012 dryness may thus have also been influenced by North Atlantic SST conditions.

Natural states of SST forcing represent one contributing factor to the recent drought events and may provide the best prospects for long-lead drought prediction. However, the spread of the PDFs in Fig. 12 is considerable and caused by an appreciable intensity of internal atmospheric variations even on annual time scales, which limits the long-lead predictability. The thin gray bars superposed on the PDFs of Fig. 12 estimate the soil moisture signal related to long-term climate change since 1880 (to be explained in more detail in section 8d). In all years, a dry signal is evident but having a magnitude that is at least an order of magnitude weaker than the intensity of the observed drought events.

c. Diagnosis of contiguous U.S. drought variability during 1979–2012

Contiguous U.S. drought variability is diagnosed for the observations by calculating the percent area covered with soil moisture deficits less than one standardized departure. Figure 13 shows the resulting monthly time series (brown shading) for the period January 1979 through December 2012. The individual regional drought events that were diagnosed in the previous subsection can be readily identified as peaks in the time-evolving U.S. drought coverage. Also evident is an overall enlarged drought coverage during 1999–2012 compared to the preceding period of 1979–98. A similar shift toward increased U.S. drought was also evident in the PC time series of the leading EOF of monthly soil moisture (see Fig. 8).

Superposed on the plot of the observed drought time series are results of the same calculation using soil moisture from the various forced climate simulations. Drought areas are calculated for the ensemble members, and Fig. 13 shows the ensemble means of these for the CAM4 (blue curve), ECHAM5 (red curve), and ECHAM5-preindustrial (PI) simulations (green curve). There are several features of the model simulations that provide insight into interpreting the observed drought time series. First, the three models are generally in strong agreement with each other concerning the time evolution of U.S. drought signals. Second, the rather abrupt observed increase in U.S. drought coverage after the late 1990s is well captured by the models, indicating this to be a forced signal. Throughout the 1999–2012 period, all three model ensembles indicate a consistently expanded drought coverage relative to the 1979–98 period. Indeed, very few episodes of drought events before 1999 induce a U.S. areal extent of drought comparable to the sustained high coverage that exists post 1998.

A third feature of significance is that the two time series of U.S. drought coverage based on the parallel ECHAM5 runs are almost indistinguishable. Recalling that the ECHAM5 runs differ from each other in that trace gases in the PI runs are set to 1880 values and SST variability is adjusted by removing the observed long-term 1880–2012 trends (section 2), their similarity suggests that the time variability of U.S. drought since 1979 has not been appreciably determined by long-term changes in forcing associated with climate change. In particular, the parallel runs permit an interpretation that the sudden increase in observed U.S. drought coverage after the late 1990s, while being strongly forced, was principally forced by natural decadal states in ocean conditions. A similar result was recently found for a study of summer central Great Plains precipitation (Hoerling et al. 2014) and in studies of post-1979 trends in North

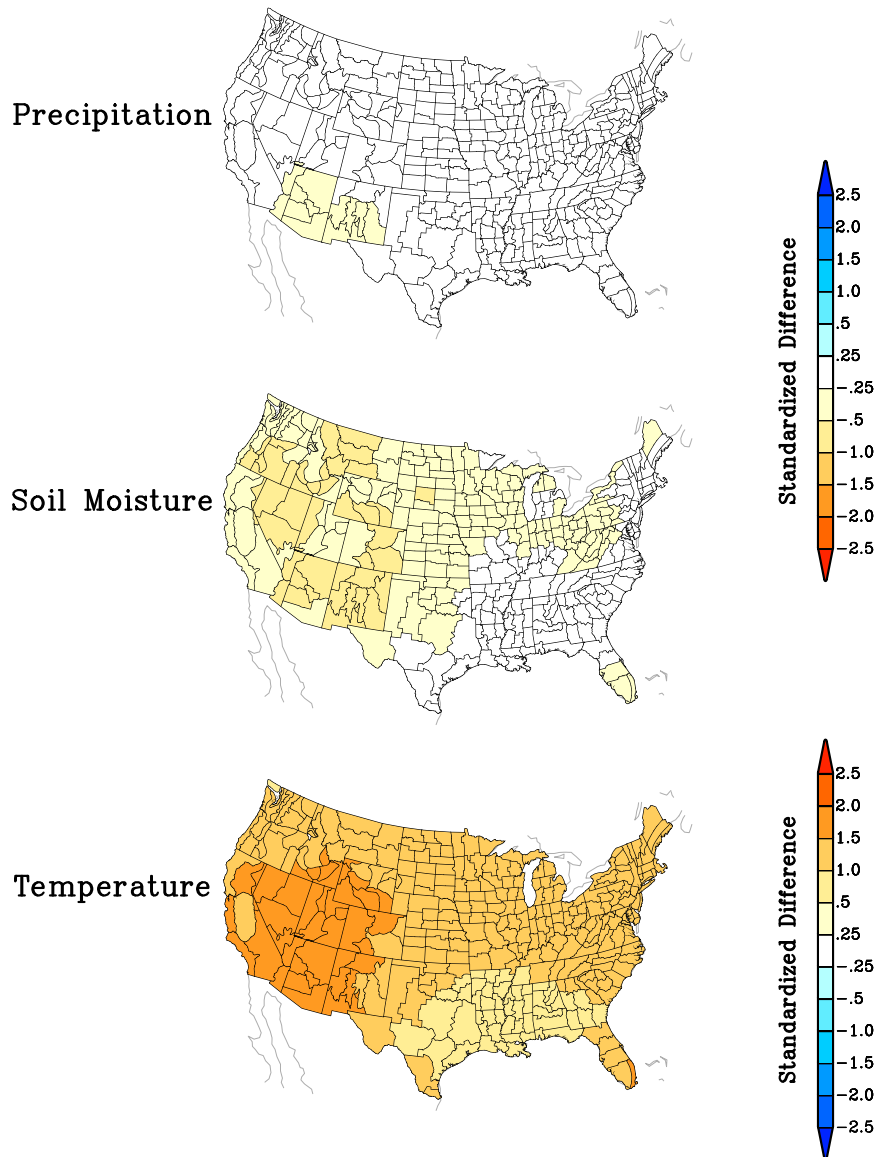


FIG. 14. Simulated long-term change in annual mean (top) climatological precipitation, (middle) soil moisture, and (bottom) surface temperature: computed from the difference between fully forced ECHAM5 simulations for 1979–2012 and the ECHAM5-PI runs in which trace gas forcings are set to climatological 1880 conditions and the 1880–2012 linear trend in SSTs is removed from the monthly SST variability.

American hydroclimate (Hoerling et al. 2010; Seager and Vecchi 2010). This drying over recent decades is consistent with the warm state of the North Atlantic Ocean (which developed after the late 1990s) and the overall cool state of the tropical Pacific since the 1997/98 El Niño (e.g., Schubert et al. 2009; Kushnir et al. 2010).

d. Climate change forcing of U.S. droughts during 1979–2012

Next we pose the question of how large the human-influence on U.S. drought may have been, when referenced

to a longer period of the climate record. The diagnosis involves intercomparison of the two parallel 10-member ensembles of ECHAM5 experiments. Shown in Fig. 14 is the difference between their annual mean climatological precipitation (top), soil moisture (middle), and surface air temperature (bottom). Further, the LTC bars of Fig. 12 are the result of averaging the mean changes in soil moisture, shown in Fig. 14 (middle panel), over each of the respective drought regions. The cause for the differences in Fig. 12 is entirely due to the model's sensitivity to the change in global sea surface

temperature and external radiative forcing since 1880. A weak signal of reduced annual precipitation (0.25 standardized departure of the variability in annual precipitation) occurs over the U.S. Southwest, with virtually no mean precipitation signal over other portions of the United States. This is quite consistent with the regional-scale drying signal in the southwest United States projected in the Coupled Model Intercomparison Project (CMIP) phase 3 and 5 simulations (e.g., Seager et al. 2007, 2013) to begin in the late twentieth century and strengthen over the current century but, as of now, to be of modest strength. Hence, insofar as the drought events in 1988, 2000, 2011, and 2012 were principally the consequence of failed rains, and not centered in the U.S. Southwest, this assessment indicates that long-term climate change was not likely a substantial player for these events.

Soil moisture is also sensitive to temperature, however, and the model simulations reveal a strong warming of U.S. annual temperatures in response to the long-term change in forcing since the late nineteenth century (Fig. 14, bottom). The strongest signal occurs, once again, over the U.S. Southwest where the simulated warming magnitude is 1.5–2.0 standard deviations of the annually averaged variability. Warming of weaker magnitude is simulated over much of the remaining United States, with a distinct minimum over the southeast United States. This spatial pattern of temperature change, with strong magnitude over the U.S. Southwest, is quite consistent with that observed over the last century (Hoerling et al. 2013a).

Principally as a consequence of this warming, the model soil moisture declines over most of the western and northern United States, with magnitudes mostly near 0.25 standardized departures (Fig. 14, middle). The implied increase in area coverage of low soil moisture over the United States as a whole is qualitatively consistent with an estimated increase in the area affected by severe to extreme drought over the United States during 1950–2006 (Easterling et al. 2007). The empirical estimates of long-term change have relied on analysis of long-term trends in the Palmer drought severity index, yet that index is known to exaggerate the deterioration of surface moisture conditions in response to temperature warming (e.g., Milly and Dunne 2011; Hoerling et al. 2012). It is therefore difficult to verify the quantitative veracity of simulated long-term soil moisture change from observations alone. However, the magnitude of the ECHAM5 simulated signal is consistent with results from soil moisture responses in CMIP3 models that show limited changes to date (Sheffield and Wood 2008).

To answer the question of how large the contribution of human-induced climate change was during the severe

drought events of 1988, 2000, 2011, and 2012, we spatially average the simulated long-term soil moisture changes over the prior assessed four drought regions. The thin gray bars on the PDFs of Fig. 12 summarize the results. In all cases, the estimated long-term change signal is about an order of magnitude smaller than the event magnitude itself. Note furthermore that the magnitude of the long-term climate change signal to date is small compared to the spread of each PDF, attesting both to its small role relative to natural internal variability of the atmosphere alone and to its limited detectability as of now, consistent with the conclusions of Sheffield and Wood (2008). Lastly, it is instructive to compare how large the current climate change signal is relative to a signal associated with natural oceanic boundary forcings. For the 2011 and 2012 droughts, for instance, the natural ocean-forced signal is about a factor of 5 greater than the signal of long-term change. It is also important to emphasize that the long-term climate change signal does not inform one as to when severe droughts are likely to occur, whereas time-evolving natural states of the oceans can. Useful interannual predictability of drought events for specific locations thus continues to hinge critically on the predictability of such natural variations in ocean states. An intriguing aspect of the estimated long-term change in soil moisture due to global warming (Fig. 14) is that owing to a regional specificity in signal—with greater temperature rises over the southwestern United States together with greater reduction in precipitation—drought events there are likely to be more severe now and sustained compared to events elsewhere in the United States.

9. Conclusions

We have reviewed various lines of evidence for the origins of North American drought variability over the last century, with a more detailed examination of U.S. drought variability during the last three decades. While this assessment introduces several new model simulations updated to include recent (2012) conditions, it incorporates methods (AMIP-style simulations with large ensembles) that have been widely utilized in numerous prior investigations on factors causing drought. Integrating these new experiments with the extensive literature, the following synthesis of the various factors responsible for North American drought is offered:

- Generation by SST variability of atmospheric circulation anomalies that affect precipitation over North America accounts for a modest fraction of annual mean precipitation variability. Up to 40% of annual mean precipitation variability in northeastern Mexico, Texas, the southern Great Plains, and the Gulf Coast states is caused

- by ocean forcing, but less than 20% of the variability is SST driven across much of the remainder of North America, with the weakest ocean influence occurring over central and eastern Canada. While the ocean-forced component is potentially predictable (e.g., related to ENSO) and hence receives much deserved attention, the assessment implies that even perfect SST prediction would likely capture much less than half the total variance in annual precipitation over North America.
- In spite of the modest role of the ocean variability in conditioning overall North American hydroclimate variability, the observed time histories of annual mean precipitation since 1901 in select regions—especially the southern Great Plains and southwest North America—can be reproduced with notable fidelity within atmosphere models forced by observed SSTs. Individual wet and dry years as well as extended droughts and pluvials can be simulated in this way even if the detailed time evolution or extreme magnitude of such events cannot. In this case the ocean forcing can be considered as an effective nudging influence on the atmosphere, creating at times conditions conducive for droughts (or pluvials), while internal atmospheric variability either amplifies or opposes the SST-forced signal.
 - Ocean nudging of the atmospheric state was a contributing factor in the multiyear southern U.S. droughts of the 1950s and at the turn of the century. However a striking exception is the 1973–75 period when an extended La Niña generated a severe and sustained southern U.S. drought in the model simulations but no such drought occurred in nature, most probably due to opposing and overwhelming influences of internal atmospheric variability. While biases in SST sensitivity within the current state-of-the-art atmospheric models cannot be discounted, the assessment of model and observational data points to a commonality of strong ENSO sensitivity, a potentially modest sensitivity to tropical Atlantic conditions, but only weak overall sensitivity to other oceanic conditions.
 - Estimated U.S. soil moisture variability since 1979 exhibits a similar relationship to SST variability that was found to occur for North American precipitation variability for the longer historical record since 1901. The temporal and regional articulations of several severe droughts since 1979 were significantly conditioned by SST forcing, most notably the southeast drought of 2000, the Texas drought of 2011, and the central Great Plains drought of 2012. In the case of the severe northern Great Plains drought of 1988, no appreciable SST conditioning appeared to occur, and that event most likely resulted primarily from internal atmospheric variability. Even in the other three events, the ocean-forced signal of low soil moisture was typically a factor of 2 weaker than the observed soil moisture deficits, affirming again that a complete explanation of these droughts must invoke not just the ocean forcing but also the particular sequence of internal atmospheric variability—weather—during the event.
 - Temporal variability of estimated contiguous U.S. soil moisture shows a sharp decrease in the late 1990s, and the percentage of the United States experiencing moderate to severe drought suddenly increased and remained at elevated levels during the first decade of the twenty-first century. Atmospheric climate models simulate this abrupt change quite well as a response to changes in SSTs. Our assessment of known SST relationships with U.S. drought and a diagnosis of additional climate simulations that exclude long-term trends in boundary and external radiative forcing leads to a conclusion that natural modes of decadal SST variability have been of primary importance. This includes a cooling of the tropical Pacific associated with increased occurrences of La Niña events post 1998 and an enhanced decadal warming of the tropical North Atlantic, both conditions conducive for reduced U.S. precipitation, increased surface temperature, and reduced soil moisture.
 - Diagnosis of model simulations of the effects of long-term changes in observed global SSTs, sea ice, and trace gas concentrations since 1880 indicate a strong signal of U.S. warming having maximum amplitude over the southwestern United States consistent in spatial pattern and magnitude with historical observations. The warming leads to a simulated long-term reduction in soil moisture, which, although of weak magnitude compared to soil moisture deficits induced by naturally occurring droughts in the southwest United States, would imply that drought conditions may be entered more quickly and alleviated more slowly owing to long-term warming. Long-term annual mean precipitation changes in response to changes in radiative forcing are small and mostly undetectable at this time compared to natural variability.
- To conclude, North America has an impressive, varied, and never-ending history of droughts. Much of this history can be explained in terms of forcing of atmospheric circulation anomalies from the tropical Pacific and Atlantic Oceans. This component is potentially predictable although tropical Pacific predictability is limited to at most one year and tropical Atlantic predictions essentially rely on persistence. SST prediction can provide some measure of atmospheric prediction though more so in the winter than the summer half year. In addition, the details of any one drought or any one year will be heavily influenced by internal atmospheric variability that is unpredictable beyond the time scale of

numerical weather prediction. Such atmosphere-only variability lends the extreme character to particular events like the droughts of 2011 and 2012, even though these were at least in some way influenced by La Niña conditions and can, on occasion, prevent a widespread drought occurring even when ocean conditions were apparently ripe to generate a drought, as in 1973–75. As such, drought predictability will remain limited for the foreseeable future, and probably forever. Radiative forcing of the climate system is another source of predictability, although not really a welcome one, and rising greenhouse gases will lead to a steady drying of southwest North America. However, this is a change that is only now beginning to emerge and currently is exerting less influence on precipitation variability than ocean variability or internal atmospheric variability.

Acknowledgments. The authors thank two anonymous reviewers for detailed criticisms that led to an improved paper. RS was supported by NOAA Awards NA10OAR4310137 (Global Decadal Hydroclimate Variability and Change) and NA08OAR4320912. We thank Jennifer Nakamura for conducting statistical analyses and preparing figures, Naomi Henderson and Dong Eun Lee for conducting the CCM3 integrations, Dr. XiaoWei Quan and Phil Pegen for various model simulations and Jon Eischeid for data analysis, and the NOAA Climate Program Office for support.

REFERENCES

- Bates, G. T., M. P. Hoerling, and A. Kumar, 2001: Central U.S. springtime precipitation extremes: Teleconnections and relationships with sea surface temperature. *J. Climate*, **14**, 3751–3766, doi:10.1175/1520-0442(2001)014<3751:CUSSPE>2.0.CO;2.
- Bonsal, B. R., and M. Regier, 2007: Historical comparison of the 2001/2002 drought in the Canadian Prairies. *Climate Res.*, **33**, 229–242, doi:10.3354/cr033229.
- , E. E. Wheaton, A. C. Chipanshi, C. Lin, D. J. Sauchyn, and L. Wen, 2011: Drought research in Canada: A review. *Atmos.–Ocean*, **49**, 303–319, doi:10.1080/07055900.2011.555103.
- Cai, W., and T. Cowan, 2007: Trends in Southern Hemisphere circulation in IPCC AR4 models over 1950–99: Ozone depletion versus greenhouse forcing. *J. Climate*, **20**, 681–693, doi:10.1175/JCLI4028.1.
- Chen, P., and M. E. Newman, 1998: Rossby wave propagation and the rapid development of upper-level anomalous anticyclones during the 1988 U.S. drought. *J. Climate*, **11**, 2491–2504, doi:10.1175/1520-0442(1998)011<2491:RWPATR>2.0.CO;2.
- Compo, G., and Coauthors, 2011: The Twentieth Century Reanalysis Project. *Quart. J. Roy. Meteor. Soc.*, **137**, 1–28, doi:10.1002/qj.776.
- Cook, B., R. Miller, and R. Seager, 2008: Dust and sea surface temperature forcing of the 1930s “Dust Bowl” drought. *Geophys. Res. Lett.*, **35**, L08710, doi:10.1029/2008GL033486.
- , —, and —, 2009: Amplification of the North American “Dust Bowl” drought through human-induced land degradation. *Proc. Natl. Acad. Sci. USA*, **106**, 4997–5001, doi:10.1073/pnas.0810200106.
- , E. Cook, K. Anchukaitis, R. Seager, and R. Miller, 2011a: Forced and unforced variability of twentieth century North American droughts and pluvials. *Climate Dyn.*, **37**, 1097–1110, doi:10.1007/s00382-010-0897-9.
- , R. Seager, and R. Miller, 2011b: Atmospheric circulation anomalies during two persistent North American droughts: 1932–39 and 1948–57. *Climate Dyn.*, **36**, 2339–2355, doi:10.1007/s00382-010-0807-1.
- Cook, E. R., R. Seager, M. A. Cane, and D. W. Stahle, 2007: North American droughts: Reconstructions, causes and consequences. *Earth Sci. Rev.*, **81**, 93–134, doi:10.1016/j.earscirev.2006.12.002.
- Douglas, A. V., and P. J. Englehart, 1996: Variability of the summer monsoon in Mexico and relationships with drought in the United States. *Proc. 21st Annual Climate Diagnostics and Prediction Workshop*, Huntsville, Alabama, NOAA, 296–299.
- Easterling, D. R., T. W. R. Wallis, J. H. Lawrimore, and R. R. Heim Jr., 2007: Effects of temperature and precipitation trends on U.S. drought. *Geophys. Res. Lett.*, **34**, L20709, doi:10.1029/2007GL031541.
- Enfield, D. B., A. M. Mestas-Núñez, and P. J. Trimble, 2001: The Atlantic multidecadal oscillation and its relation to rainfall and river flows in the continental U.S. *Geophys. Res. Lett.*, **28**, 2077–2080, doi:10.1029/2000GL012745.
- Findell, K. L., and T. L. Delworth, 2010: Impact of common sea surface temperature anomalies on global drought and pluvial frequency. *J. Climate*, **23**, 485–503, doi:10.1175/2009JCLI3153.1.
- Fye, F. K., D. W. Stahle, and E. R. Cook, 2003: Paleoclimatic analogs to twentieth century moisture regimes across the United States. *Bull. Amer. Meteor. Soc.*, **84**, 901–909, doi:10.1175/BAMS-84-7-901.
- Gent, P., and Coauthors, 2011: The Community Climate System Model version 4. *J. Climate*, **24**, 4973–4991, doi:10.1175/2011JCLI4083.1.
- Herweijer, C., R. Seager, and E. R. Cook, 2006: North American droughts of the mid to late nineteenth century: History, simulation and implications for mediaeval drought. *Holocene*, **16**, 159–171, doi:10.1191/0959683606hl917rp.
- Higgins, R. W., Y. Chen, and A. V. Douglas, 1999: Interannual variability of the North American warm season precipitation regime. *J. Climate*, **12**, 653–680, doi:10.1175/1520-0442(1999)012<0653:IVOTNA>2.0.CO;2.
- Hoerling, M. P., and A. Kumar, 2003: The perfect ocean for drought. *Science*, **299**, 691–694, doi:10.1126/science.1079053.
- , and S. Schubert, 2010: Oceans and drought. *Proceedings of OceanObs’09: Sustained Ocean Observations and Information for Society*, Vol. 1, J. Hall, D. Harrison, and D. Stammer, Eds., ESA WPP-306, 531–540, doi:10.5270/OceanObs09.
- , X.-W. Quan, and J. Eischeid, 2009: Distinct causes for two principal U.S. droughts of the 20th century. *Geophys. Res. Lett.*, **36**, L19708, doi:10.1029/2009GL039860.
- , J. Eischeid, and J. Perlwitz, 2010: Regional precipitation trends: Distinguishing natural variability from anthropogenic forcing. *J. Climate*, **23**, 2131–2145, doi:10.1175/2009JCLI3420.1.
- , and Coauthors, 2011: North American decadal climate for 2011–20. *J. Climate*, **24**, 4519–4528, doi:10.1175/2011JCLI4137.1.
- , J. Eischeid, X. Quan, H. Diaz, R. Webb, R. Dole, and D. Easterling, 2012: Is a transition to semipermanent drought conditions imminent in the U.S. Great Plains? *J. Climate*, **25**, 8380–8386, doi:10.1175/JCLI-D-12-00449.1.
- , M. Dettinger, K. Wolter, L. Lukas, J. Eischeid, R. Nemani, B. Liebmann, and K. E. Kunke, 2013a: Present weather and

- climate: Evolving conditions. Assessment of climate change in the southwest United States: A report prepared for the National Climate Assessment, G. Garfin et al., Eds., Southwest Climate Alliance, Island Press, 74–100.
- , and Coauthors, 2013b: Anatomy of an extreme event. *J. Climate*, **26**, 2811–2832, doi:10.1175/JCLI-D-12-00270.1.
- , J. Eischeid, A. Kumar, R. Leung, A. Mariotti, K. Mo, S. Schubert, and R. Seager, 2014: Causes and predictability of the 2012 Great Plains drought. *Bull. Amer. Meteor. Soc.*, **95**, 269–282.
- Hoskins, B., and K. Karoly, 1981: The steady response of a spherical atmosphere to thermal and orographic forcing. *J. Atmos. Sci.*, **38**, 1179–1196, doi:10.1175/1520-0469(1981)038<1179:TSLROA>2.0.CO;2.
- Huang, H.-P., R. Seager, and Y. Kushnir, 2005: The 1976/77 transition in precipitation over the Americas and the influence of tropical SST. *Climate Dyn.*, **24**, 721–740, doi:10.1007/s00382-005-0015-6.
- Huang, J., H. van den Dool, and K. Georgarakos, 1996: Analysis of model-calculated soil moisture over the U.S. (1931–1993) and applications to long-range temperature forecasts. *J. Climate*, **9**, 1350–1362, doi:10.1175/1520-0442(1996)009<1350:AOMCSM>2.0.CO;2.
- Kaplan, A., M. A. Cane, Y. Kushnir, A. C. Clement, M. B. Blumenthal, and B. Rajagopalan, 1998: Analyses of global sea surface temperature: 1856–1991. *J. Geophys. Res.*, **103**, 18 567–18 589, doi:10.1029/97JC01736.
- Kennedy, L. J., N. A. Rayner, R. O. Smith, D. E. Parker, and M. Saunby, 2011a: Reassessing biases and other uncertainties in sea surface temperature observations since 1850: 1. Measurement and sampling errors. *J. Geophys. Res.*, **116**, D14103, doi:10.1029/2010JD015218.
- , —, —, —, and —, 2011b: Reassessing biases and other uncertainties in sea surface temperature observations since 1850: 2. Biases and homogenization. *J. Geophys. Res.*, **116**, D14104, doi:10.1029/2010JD015220.
- Kiehl, J. T., J. J. Hack, G. B. Bonan, B. A. Boville, D. L. Williamson, and P. J. Rasch, 1998: The National Center for Atmospheric Research Community Climate Model: CCM3. *J. Climate*, **11**, 1131–1149, doi:10.1175/1520-0442(1998)011<1131:TNCFAR>2.0.CO;2.
- Kistler, R., and Coauthors, 2001: The NCEP–NCAR 50-Year Reanalysis: Monthly means CD-ROM and documentation. *Bull. Amer. Meteor. Soc.*, **82**, 247–267, doi:10.1175/1520-0477(2001)082<0247:TNNYRM>2.3.CO;2.
- Kushnir, Y., R. Seager, M. Ting, N. Naik, and J. Nakamura, 2010: Mechanisms of tropical Atlantic SST influence on North American hydroclimate variability. *J. Climate*, **23**, 5610–5628, doi:10.1175/2010JCLI3172.1.
- Lau, N.-C., A. Leetmaa, and M. J. Nath, 2006: Attribution of atmospheric variations in the 1997–2003 period to SST anomalies in the Pacific and Indian Ocean basins. *J. Climate*, **19**, 3607–3628, doi:10.1175/JCLI3813.1.
- L’Heureux, M. L., and D. W. J. Thompson, 2006: Observed relationships between the El Niño–Southern Oscillation and the extratropical zonal mean circulation. *J. Climate*, **19**, 276–287, doi:10.1175/JCLI3617.1.
- Liu, A. Z., M. Ting, and H. Wang, 1998: Maintenance of circulation anomalies during the 1988 drought and 1993 floods over the United States. *J. Atmos. Sci.*, **55**, 2810–2832, doi:10.1175/1520-0469(1998)055<2810:MOCADT>2.0.CO;2.
- Lyu, J., G. Chen, and D. M. W. Frierson, 2008: Response of the zonal mean atmospheric circulation to El Niño versus global warming. *J. Climate*, **21**, 5835–5851, doi:10.1175/2008JCLI2200.1.
- Lyon, B., and R. M. Dole, 1995: A diagnostic comparison of the 1980 and 1988 United States summer heat wave-droughts. *J. Climate*, **8**, 1658–1675, doi:10.1175/1520-0442(1995)008<1658:ADCOTA>2.0.CO;2.
- McCabe, G. J., M. A. Palecki, and J. L. Betancourt, 2004: Pacific and Atlantic influences on multidecadal drought frequency in the United States. *Proc. Natl. Acad. Sci. USA*, **101**, 4136–4141, doi:10.1073/pnas.0306738101.
- Milly, P. C. D., and K. A. Dunne, 2011: On the hydrologic adjustment of climate-model projections: The potential pitfall of potential evapotranspiration. *Earth Interact.*, **15**, doi:10.1175/2010EI363.1.
- Mitchell, T. D., and P. D. Jones, 2005: An improved method of constructing a database of monthly climate observations and associated high-resolution grids. *Int. J. Climatol.*, **25**, 693–712, doi:10.1002/joc.1181.
- National Research Council, 2002: *Abrupt Climate Change: Inevitable Surprises*. National Academy of Sciences, 244 pp.
- Nigam, S., B. Guan, and A. Ruiz-Barradas, 2011: Key role of the Atlantic multidecadal oscillation in 20th century drought and wet periods over the Great Plains. *Geophys. Res. Lett.*, **38**, L16713, doi:10.1029/2011GL048650.
- Palmer, T. N., and C. Brankovic, 1989: The 1988 US drought linked to anomalous sea surface temperature. *Nature*, **338**, 54–57, doi:10.1038/338054a0.
- Polvani, L. M., D. W. Waugh, G. J. P. Correa, and S.-W. Son, 2011: Stratospheric ozone depletion: The main driver of twentieth-century atmospheric circulation changes in the Southern Hemisphere. *J. Climate*, **24**, 795–812, doi:10.1175/2010JCLI3772.1.
- Rasmusson, E., and J. M. Wallace, 1983: Meteorological aspects of the El Niño–Southern Oscillation. *Science*, **222**, 1195–1202, doi:10.1126/science.222.4629.1195.
- Roeckner, E. K., and Coauthors, 2003: The atmospheric general circulation model ECHAM5. Part I: Model description. MPI Tech. Rep. 349, 127 pp. [Available online at https://www.mpimet.mpg.de/fileadmin/publikationen/Reports/max_scirep_349.pdf.]
- Ruff, T., Y. Kushnir, and R. Seager, 2012: Comparing twentieth- and twenty-first-century patterns of interannual precipitation variability over the western United States and northern Mexico. *J. Hydrometeorol.*, **13**, 366–378, doi:10.1175/JHM-D-10-05003.1.
- Schubert, S. D., M. J. Suarez, P. J. Pegion, R. D. Koster, and J. T. Bacmeister, 2004a: Causes of long-term drought in the United States Great Plains. *J. Climate*, **17**, 485–503, doi:10.1175/1520-0442(2004)017<0485:COLDIT>2.0.CO;2.
- , —, —, —, and —, 2004b: On the cause of the 1930s Dust Bowl. *Science*, **303**, 1855–1859, doi:10.1126/science.1095048.
- , —, —, —, and —, 2008: Potential predictability of long-term drought and pluvial conditions in the U.S. Great Plains. *J. Climate*, **21**, 802–816, doi:10.1175/2007JCLI1741.1.
- , and Coauthors, 2009: A U.S. CLIVAR project to assess and compare the responses of global climate models to drought-related SST forcing patterns: Overview and results. *J. Climate*, **22**, 5251–5272, doi:10.1175/2009JCLI3060.1.
- Seager, R., 2007: The turn of the century North American drought: Dynamics, global context, and prior analogs. *J. Climate*, **20**, 5527–5552, doi:10.1175/2007JCLI1529.1.
- , and G. A. Vecchi, 2010: Greenhouse warming and the 21st century hydroclimate of southwestern North America. *Proc. Natl. Acad. Sci. USA*, **107**, 21 277–21 282, doi:10.1073/pnas.0910856107.
- , N. Harnik, Y. Kushnir, W. Robinson, and J. Miller, 2003: Mechanisms of hemispherically symmetric climate variability. *J. Climate*, **16**, 2960–2978, doi:10.1175/1520-0442(2003)016<2960:MOHSCV>2.0.CO;2.

- , Y. Kushnir, C. Herweijer, N. Naik, and J. Velez, 2005: Modeling of tropical forcing of persistent droughts and pluvials over western North America: 1856–2000. *J. Climate*, **18**, 4065–4088, doi:10.1175/JCLI3522.1.
- , and Coauthors, 2007: Model projections of an imminent transition to a more arid climate in southwestern North America. *Science*, **316**, 1181–1184, doi:10.1126/science.1139601.
- , Y. Kushnir, M. Ting, M. A. Cane, N. Naik, and J. Velez, 2008: Would advance knowledge of 1930s SSTs have allowed prediction of the Dust Bowl drought? *J. Climate*, **21**, 3261–3281, doi:10.1175/2007JCLI2134.1.
- , A. Tzanova, and J. Nakamura, 2009a: Drought in the southeastern United States: Causes, variability over the last millennium and the potential for future hydroclimate change. *J. Climate*, **22**, 5021–5045, doi:10.1175/2009JCLI2683.1.
- , and Coauthors, 2009b: Mexican drought: An observational, modeling and tree ring study of variability and climate change. *Atmósfera*, **22**, 1–31.
- , N. Naik, and L. Vogel, 2012a: Does global warming cause intensified interannual hydroclimate variability? *J. Climate*, **25**, 3355–3372, doi:10.1175/JCLI-D-11-00363.1.
- , N. Pederson, Y. Kushnir, J. Nakamura, and S. Jurburg, 2012b: The 1960s drought and subsequent shift to a wetter climate in the Catskill Mountains region of the New York City watershed. *J. Climate*, **25**, 6721–6742, doi:10.1175/JCLI-D-11-00518.1.
- , M. Ting, C. Li, N. Naik, B. Cook, J. Nakamura, and H. Liu, 2013: Projections of declining surface water availability for the southwestern U.S. *Nat. Climate Change*, **3**, 482–486, doi:10.1038/nclimate1787.
- , L. Goddard, J. Nakamura, N. Henderson, and D. E. Lee, 2014: Dynamical causes of the 2010/11 Texas–northern Mexico drought. *J. Hydrometeor.*, **15**, 39–68, doi:10.1175/JHM-D-13-024.1.
- Sheffield, J., and E. Wood, 2008: Projected changes in drought occurrence under future global warming from multi-model, multi-scenario, IPCC AR4 simulations. *Climate Dyn.*, **31**, 79–105, doi:10.1007/s00382-007-0340-z.
- Son, S. W., N. F. Tandon, L. M. Polvani, and S. W. Waugh, 2009: Ozone hole and Southern Hemisphere climate change. *Geophys. Res. Lett.*, **36**, L15705, doi:10.1029/2009GL038671.
- Stahle, D. W., F. K. Fye, E. R. Cook, and R. D. Griffin, 2007: Tree ring reconstructed megadroughts over North America since AD 1300. *Climatic Change*, **83**, 133–149, doi:10.1007/s10584-006-9171-x.
- , and Coauthors, 2009: Early 21st-century drought in Mexico. *Eos, Trans. Amer. Geophys. Union*, **90**, 89–100, doi:10.1029/2009EO110001.
- Stewart, R., and R. Lawford, 2011: The 1999–2005 Canadian Prairies drought: Science, impacts, and lessons. Tech. Rep., Drought Research Initiative, 114 pp. [Available online at <http://www.meteo.mcgill.ca/dri/errata.php>.]
- Trenberth, K., G. Branstator, and P. Arkin, 1988: Origins of the 1988 North American drought. *Science*, **242**, 1640–1645, doi:10.1126/science.242.4886.1640.
- Weiss, J. L., C. L. Castro, and J. T. Overpeck, 2009: Distinguishing pronounced droughts in the southwestern United States: Seasonality and effects of warmer temperatures. *J. Climate*, **22**, 5918–5932, doi:10.1175/2009JCLI2905.1.
- Worster, D., 1979: *Dust Bowl: The Southern Plains in the 1930s*. Oxford University Press, 277 pp.
- Zhang, Y., J. M. Wallace, and D. S. Battisti, 1997: ENSO-like decade-to-century scale variability: 1900–93. *J. Climate*, **10**, 1004–1020, doi:10.1175/1520-0442(1997)010<1004:ELIV>2.0.CO;2.